University of Alabama at Birmingham
UAB Digital Commons

All ETDs from UAB | UAB Theses & Dissertations

1975

Binding Of 1,N(6)-Ethenoadenosine Triphosphate To Actin Fluorescence Emission Properties.

Kenneth Edwin Thames
University of Alabama at Birmingham

Follow this and additional works at: https://digitalcommons.library.uab.edu/etd-collection

Recommended Citation

Thames, Kenneth Edwin, "Binding Of 1,N(6)-Ethenoadenosine Triphosphate To Actin Fluorescence Emission Properties." (1975). *All ETDs from UAB*. 4005.
https://digitalcommons.library.uab.edu/etd-collection/4005

This content has been accepted for inclusion by an authorized administrator of the UAB Digital Commons, and is provided as a free open access item. All inquiries regarding this item or the UAB Digital Commons should be directed to the UAB Libraries Office of Scholarly Communication.

INFORMATION TO USERS

This material was produced from a microfilm copy of the original document. While the most advanced technological means to photograph and reproduce this document have been used, the quality is heavily dependent upon the quality of the original submitted.

The following explanation of techniques is provided to help you understand markings or patterns which may appear on this reproduction.

1. The sign or "target" for pages apparently lacking from the document photographed is "Missing Page(s)". If it was possible to obtain the missing page(s) or section, they are spliced into the film along with adjacent pages. This may have necessitated cutting thru an image and duplicating adjacent pages to insure you complete continuity.

2. When an image on the film is obliterated with a large round black mark, it is an indication that the photographer suspected that the copy may have moved during exposure and thus cause a blurred image. You will find a good image of the page in the adjacent frame.

3. When a map, drawing or chart, etc., was part of the material being photographed the photographer followed a definite method in "sectioning" the material. It is customary to begin photoing at the upper left hand corner of a large sheet and to continue photoing from left to right in equal sections with a small overlap. If necessary, sectioning is continued again — beginning below the first row and continuing on until complete.

4. The majority of users indicate that the textual content is of greatest value, however, a somewhat higher quality reproduction could be made from "photographs" if essential to the understanding of the dissertation. Silver prints of "photographs" may be ordered at additional charge by writing the Order Department, giving the catalog number, title, author and specific pages you wish reproduced.

5. PLEASE NOTE: Some pages may have indistinct print. Filmed as received.

Xerox University Microfilms

300 North Zeeb Road
Ann Arbor, Michigan 48106

76-7800

THAMES, Kenneth Edwin, 1943-
BINDING OF 1,N^6-ETHENOADENOSINE TRIPHOSPHATE TO ACTIN FLUORESCENCE EMISSION PROPERTIES.

The University of Alabama in Birmingham Medical Center, Ph.D., 1975
Biophysics, general

Xerox University Microfilms, Ann Arbor, Michigan 48106

© 1975

KENNETH EDWIN THAMES

ALL RIGHTS RESERVED

BINDING OF 1,N^6-ETHENOADENOSINE TRIPHOSPHATE TO ACTIN

FLUORESCENCE EMISSION PROPERTIES

by

KENNETH EDWIN THAMES

A DISSERTATION

Submitted in partial fulfillment of the requirements for the degree of Doctor of Philosophy in the Department of Physiology and Biophysics in The Graduate School, University of Alabama in Birmingham

Birmingham, Alabama

1975

ACKNOWLEDGEMENTS

I would like to express my sincere appreciation to my wife, Shirley, whose steadfast support made my studies possible.

I want to thank Dr. H. C. Cheung for his guidance and patience during the course of my graduate studies.

I also express my appreciation to Dr. S. C. Harvey for his guidance and assistance throughout these studies.

TABLE OF CONTENTS

Table of Contents (continued)

LIST OF TABLES

LIST OF FIGURES

List of Figures (continued)

List of Figures (continued)

I. INTRODUCTION

A. Actin and the Contractile Apparatus

A muscle cell contains not only a contractile structure, but also a contractile regulatory structure and a structure to supply energy. The interior of the muscle cell is divided into the contractile structure called myofibrils, and sarcoplasm. The longitudinal cross section of myofibrils as seen under an optical microscope are striated with repeat units about every 2.5 μ. The light bands are called isotropic or I bands; the dark bands are called anisotropic or A bands. The I bands are dissected by a dense transverse line called the Z line or Z band. The central portion of the A band, which is called the H zone is less dense than the rest of the band; it is bisected by a transverse dense line, the M line. The longitudinal repeat unit from Z line to Z line is called a sarcomere. The I band contains the thin filaments composed primarily of the protein actin along with tropomyosin and troponin.

In vitro actin, the major protein of the thin filaments of muscle, can exist in two forms, G-actin and F-actin (Figure 1). G-actin is a globular protein of molecular weight 46,000 daltons with a low degree of asymmetry (Cheung et al., 1971). The complete amino acid sequence of rabbit skeletal muscle actin has been worked

FIGURE 1

Organization of thin filament showing the assembly of actin, tropomyosin and troponin molecules.

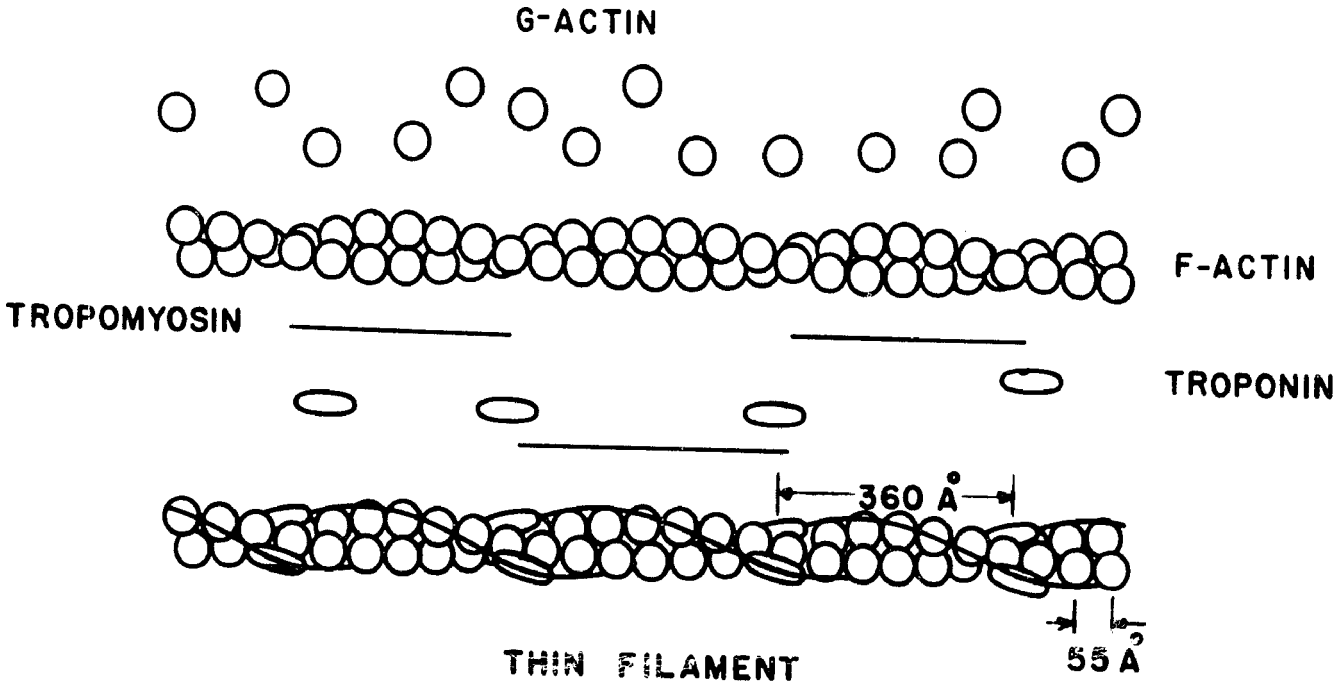

ORGANIZATION OF THIN FILAMENT

out by Elzinga et al. (1973). The actin polypeptide chain is composed of 374 residues, including one residue of the unusual amino acid, N-methyl histidine. G-actin binds one Ca^{++} or Mg^{++} ion and one adenosine triphosphate (ATP), both of which are necessary to stabilize the actin structure.

On addition of neutral salts, the monomeric G-actin is transformed into a long fibrous polymer called F-actin having a particle weight frequently in excess of several million daltons. The polymerization of G-actin to F-actin results in the dephosphorylation of the bound ATP to bound adenosine diphosphate (ADP). F-actin consists of two strands of G-actin monomers in a double helical string of beads configuration.

Actin of the thin filament is closely associated with two other proteins, tropomyosin and troponin, whose function is associated with regulation of muscle contraction (Ebashi and Endo, 1968).

The protein composition of the thin filaments includes two additional minor proteins, β-actinin (Maruyama, 1965) and α-actinin. The function of β-actinin is still obscure. It appears to be a length determining factor for the thin filaments. It has also been reported that G-actin polymerized in the presence of this protein results in an unstable F-actin (Maruyama, 1973). The other minor protein, α-actinin, is located at the Z membrane of myofibrils (Masaki et al., 1967). Evidence indicates that α-actinin has a cross-linking action on F-actin (Goll et al., 1972; Abe and Maruyama, 1973).

Tropomyosin is a helical double stranded rodlike molecule of molecular weight 68,000 daltons and length 450 Å (Taylor, 1972). The tropomyosin molecules attach end-to-end forming a thin thread that lies near the groove between the paired actin strands (Figure 1). The interaction of actin with tropomyosin has been demonstrated by viscometric methods (Tonomura, 1973). The function of tropomyosin resides in its cooperative action with the globular protein, troponin, to regulate the binding of actin with myosin. Tropomyosin senses calcium binding by the troponin and releases its inhibition of the attachment of myosin cross-bridges to actin. There are a number of models for the process, all of which assume that binding of calcium causes a structural change in the troponin-tropomyosin complex. Some believe that the change in the troponin complex directly alters the position of the tropomyosin strands, thereby exposing the active sites on actin which previously had been blocked (H. E. Huxley, 1973); others suggest that the change acts more directly on the configuration of the active site on the actin itself, and that the tropomyosin serves as a messenger to distribute the information to the seven actins with which it is associated (Ohtsuki et al., 1967; Bremel and Weber, 1972). Whatever the mechanism of regulation, the actin becomes free to complex with structures of the thick filament when Ca^{++} is available.

Myosin, the major protein of the thick filament, is a long asymmetric molecule containing two globular heads (Figure 2). The total length of the myosin molecule is 1600 Å, and it has a number-average molecular weight of about 470,000 daltons (Tonomura et al.,

FIGURE 2

Myosin and the thick filament.

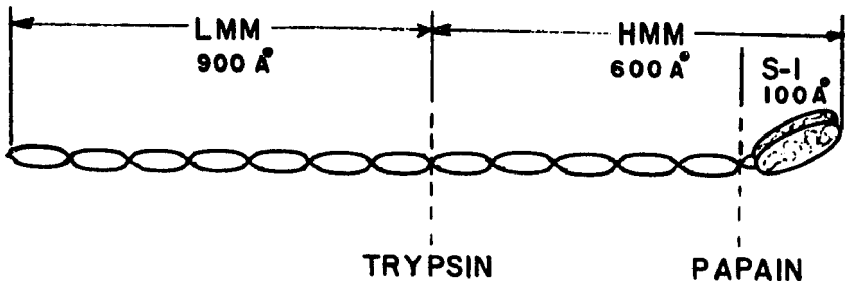

MYOSIN

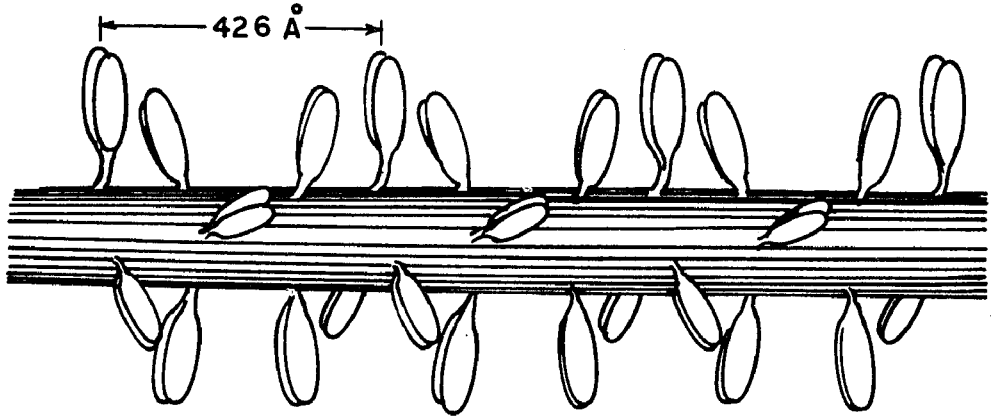

THICK FILAMENT

(1966). Treatment of one mole of myosin with trypsin or chymotrypsin yields one mole of heavy meromyosin (HMM) and one mole of light meromyosin (LMM) (Szent-Gyorgyi, 1953). Further digestion of HMM with trypsin yields a smaller active subfragment, S-1 (Mueller and Perry, 1962). This fragment has the ability to bind F-actin and contains the ATPase active site of myosin. Papain can also split off the enzymatic globular regions (S-1) of myosin. The globular heads (S-1) of the myosin molecules protrude out from the body of the thick filament forming the cross-bridges. Two additional proteins are associated with the myosin in the thick filaments, M-protein (Masaki and Takaiti, 1974) constitutes the M-line of myofibrils. It binds rather firmly to myosin, but its function is unknown. Another protein, C-protein, (Starr and Offer, 1971) also binds strongly to myosin at low ionic strength. One possible function for C-protein might be that of a core protein facilitating the packing together of the tails of myosin molecules to form the backbone of the thick filament. X-ray diffraction studies of live striated vertebrate muscle showed two bridges projecting out directly opposite each other from the backbone of the thick filament. The next two bridges occurred 143 $\mathring{A}$ further along the filament and were rotated relative to the first pair by 122 degrees (Huxley, 1969). The myosin molecules are arranged with opposite structural polarity on each side of the midpoint of the filament. The actin molecules are arranged in the thin filaments with appropriate polarity to interact with the nearby myosin heads.

The generally accepted model for this interaction between thick and thin filaments leading to muscle contraction is the sliding filament model of H. Huxley and Hanson (1954) and of A. Huxley and Niedergerke (1954). The contraction of striated muscle is brought about by some mechanism which generates a relative sliding force between the partly overlapping arrays of thin and thick filaments (Figure 3). The cross-bridges projecting out from the myosin filaments, and carrying the adenosine triphosphatase and actin binding sites, are believed to be involved in this force generation in some cyclical process. Contraction is regulated by the troponin-tropomyosin complex attached to the actin filament. Activation of muscle results in the release of Ca^{++} by the sarcoplasmic reticulum. The Ca^{++} binds to the troponin-tropomyosin complex releasing the inhibition of this system and allowing actin to bind with the myosin cross-bridges resulting in force generation and shortening of the muscle. Relaxation results from an uptake of the Ca^{++} from the troponin by the sarcoplasmic reticulum with the concomitant conformational change blocking the interaction of actin with myosin.

B. Nature of Actin-Bound Nucleotides

G-actin is polymerized reversibly to F-actin by the addition of neutral salts. While ATP bound to G-actin exchanges readily with free-ATP, ADP bound to F-actin is not readily exchangeable. The extent of exchangeability of ADP bound to F-actin is increased

FIGURE 3

Striated pattern of muscle fiber with arrangement of thick and thin filaments.

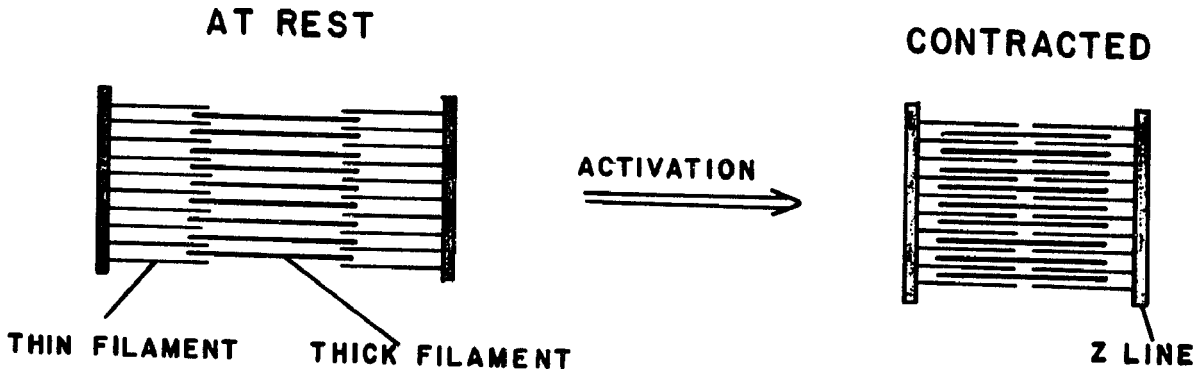
AT REST
CONTRACTED
ACTIVATION
THIN FILAMENT
THICK FILAMENT
Z LINE

by sonication (Asakura et al., 1963), and decreased in the presence of tropomyosin or myosin (Kasai and Oosawa, 1969).

West (1970b) found that the absorbance of ADP·G-actin differed from that of actin prepared in inosine triphosphate (ITP) or ATP. While absorbance changes cannot be taken as proof of conformational change, the absorbance change which results when actin-bound ADP was replaced by ATP may reflect a conformational change close to tyrosine and tryptophane residues of the actin. In contrast, Higashi and Oosawa (1965) found no appreciable difference in absorption spectra between G-actin having bound ADP and that having bound ATP or ITP, which show different rates of polymerization. They found that the polymerization of G-actin to F-actin is accompanied by a large change in ultraviolet absorption. They concluded from their analysis of the different spectra that during polymerization some of the tryptophane and tyrosine residues exposed outside are folded inside the molecule, and the conformation of the peptide chain is also changed. Binding and exchange studies suggest that the base and the phosphate chain are important, as well as the ribose-OH group in the binding of actin with nucleotide.

Varied chemical modification of actin has been performed to elucidate its function and binding characteristics. The addition of ethylenediaminetetraacetate (EDTA) to G-actin liberates bound ATP and Ca^{++}, alters its conformation, and suppresses its polymerization. However, addition of EDTA to F-actin induces very little depolymerization. Sulfhydryl reagents have been used to study the complexing of actin with ATP (Tonomura, 1973).

P-Chloromercuribenzoate (PCMB) removes Ca^{++} from actin when it binds the SH groups of actin. As pointed out by Tonomura (1973), the action of EDTA and PCMB on G-actin can be explained reasonably by Strohman and Samorodin's model (1962) of the binding of G-actin with ATP. Adenosine binds to an SH group, while the triphosphate group is thought to chelate a Ca^{++} ion strongly bound to the G-actin. In this model ATP will be removed whether PCMB binds with the SH or EDTA removes the Ca^{++}. This model can account for the observations of West (1971) with ATP and ADP and those of Thames et al. (1974) with an ATP analog. The binding constant of cation-free actin for ATP, ADP, and the ATP analog is approximately one thousandth that of the constant for ATP in the presence of bound cation, while binding of ATP is appreciably higher than of ADP when cation is present. This model, however, cannot account for the changes that occur in the actin structure. Recently experiments by Muszbek and Laki (1974) suggested that the terminal phosphate of ATP in G-actin is bound to two arginine residues. This conclusion results from their observation that thrombin splits F-actin faster than G-actin. Thrombin is specific for arginine residues, and if the terminal phosphate of ATP is bound to arginine residues the terminal phosphate will prevent these two arginine residues from being attached to thrombin's specificity site. The terminal phosphate is absent in F-actin and thus thrombin can attach to the two arginine residues and split the peptide bond at these residues.

The functions of the nucleotide bound to actin observed so far are the stabilizing effect of bound ATP on G-actin and its regulation of the rate of actin polymerization. Higashi and Oosawa (1965) showed that the polymerization rate of actin increases in the order: G-actin without nucleotide, G-actin having ADP, and G-actin having ATP. G-actin devoid of nucleotides loses polymerizability very rapidly. Kasai et al. (1965) succeeded in stabilizing this G-actin with adding a high concentration of sucrose and polymerizing it by salts without the participation of nucleotides. Barany et al. (1966) used activated charcoal to remove 90% of the bound nucleotide of F-actin. This F-actin depolymerized reversibly and complexed with myosin. Therefore, the removal of nucleotides from actin does not affect its function, but modifies the actin structure making it more stable and rendering it favorable for polymerization.

C. $1,N^6$-ethenoadenosine Triphosphate as a Probe for Actin

Fluorescence emission was the primary experimental research tool in this study. The fluorescence, in general, of a protein molecule can originate from: (1) intrinsic chromophores of proteins. These are the aromatic side chains of phenylalanine, tyrosine, and tryptophane. However, these residues may not be in an interesting site in the protein; (2) extrinsic chromophores may be inserted into the protein of interest; (3) a small proportion of proteins also contain a fluorescent coenzyme such as

reduced nicotinamide-adenine dinucleotide. There are some requirements for the optimum use of an extrinsic chromophore: (1) it should be bound to the protein at a biologically interesting location; (2) the fluorescence properties of the probe should be sensitive to the structure and dynamics of its environment in ways that are amenable to interpretation; (3) insertion of the probe should not appreciably disturb those features of the protein that are being investigated (Stryer, 1968).

The recent availability of a fluorescent ATP analog, $1,N^6$-ethenoadenosine triphosphate, εATP, (Secrist et al., 1972a) with its absorption and emission properties compatible for study of proteins suggested the possibility of using this analog to study the interaction of actin with myosin. εATP (Figure 4) is obtained by reacting ATP with chloroacetaldehyde under slightly acidic conditions. The insertion of the etheno bridge makes the analog fluorescent.

Spencer et al. (1974) showed from studies of the fluorescent emission of $1,N^6$-ethenoadenosine monophosphate (εAMP) that the unprotonated (at N-9) form of εAMP is responsible for fluorescent emission while the protonated form shows little or no fluorescence. Several groups (Secrist et al., 1972a; Miki et al., 1974) have demonstrated that εATP can replace ATP in a number of enzyme systems. If the εATP binds to actin as does ATP while allowing the actin to maintain its biological function, then it should serve as a useful probe of the nucleotide cofactor of actin as well as the interaction of actin with myosin.

FIGURE 4

$1,N^6$-ethenoadenosine triphosphate (εATP).

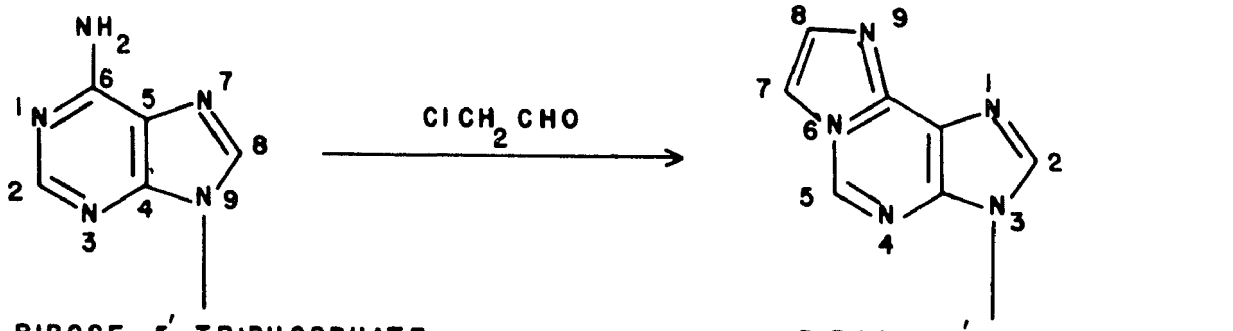
NH2
6
5
7
1
N
8
2
N
4
N
9
3
RIBOSE 5'-TRIPHOSPHATE
ClCH2CHO
8
N
9
7
1
N
6
N
2
5
N
N
3
4
RIBOSE 5'-TRIPHOSPHATE

ATP

ε-ATP

II. OBJECTIVE

In view of the differing evidence on the role of actin in muscle contraction as discussed under Introduction, it was decided to examine certain aspects of the behavior of actin with a sensitive molecular probe that can be inserted into its cofactor site. This research was undertaken to examine the possibility of replacing ATP with $1,N^6$-ethenoadenosine triphosphate (εATP) in the actin system and of using the emission properties of the bound nucleotide analog to probe the behavior of this protein.

III. MATERIALS AND METHODS

A. Reagents and Chemicals

All reagents were prepared from reagent grade chemicals. ATP in the form of sodium salt was obtained from Sigma Chemical Company. Chloroacetaldehyde was obtained by refluxing chloroacetaldehyde dimethyl acetal (Aldrich) in 50% H_2SO_4 for 45 minutes (Secrist et al., 1972b). The entire mixture was then evaporated in a rotary evaporator under reduced pressure into a flask immersed in a dry ice-acetone dewar. The colorless aqueous layer of the distillate was recovered, adjusted to pH 4.5, and redistilled. The distillate was aqueous chloroacetaldehyde (1.0 - 1.6 M). Commercial chloroacetaldehyde contained some polymeric materials and was not pure enough for the synthesis of εATP. $1,N^6$-etheno-adenosine triphosphate was synthesized by condensing ATP with 1.0 - 1.6 M chloroacetaldehyde at pH 4.0 - 4.5 at room temperature for about 24 hours (Secrist et al., 1972b). The completion of the reaction was followed by thin layer chromatography [Eastman Chromogram cellulose sheets using isobutyric acid-NH_4OH-H_2O (75:1:24, v/v)] and by monitoring the ratio of the absorption peaks 265 nm/275 nm in the ultraviolet absorption spectrum. The εATP was then decolorized with activated charcoal, if necessary, and evaporated to dryness under reduced pressure. Reprecipitation

from aqueous ethanol followed by an ethanol wash yielded εATP. Anal. calculated for $C_{12}H_{14}N_5O_{13}P_3Na_2 \cdot 3H_2O$: C, 23.08; H, 3.24; Found: C, 22.94; H, 3.69. At pH values above 4 the ultraviolet absorption spectrum of εATP in the region above 250 nm shows two major peaks, one at 265 and the other at 275 nm, with a shoulder centered around 310 nm. It is the absorption band peaking at 310 nm that is responsible for the emission properties of this compound (Spencer et al., 1974). The concentration of εATP was determined from its absorbance at 275 nm using a molar extinction of 5.6×10^3 (Secrist et al., 1972b).

B. Protein Preparations

Except as indicated, all steps involved in the preparation of actin, myosin and heavy meromyosin were carried out in a 4°C cold room. An acetone dried muscle powder was prepared from rabbit skeletal muscle by the method of Carsten and Mommaerts (1963). Actin was extracted from the acetone powder with 0.2 mM ATP adjusted to pH 7.6 and 0°C. The extraction must be carried out at 0°C in order to minimize contamination by tropomyosin (Drabikowski and Gergely, 1962). The crude extract was filtered through No. 1 Whatman filter paper and the filtrate was clarified by centrifugation at 65,000 g for 30-60 minutes. The actin thus obtained was in the monomeric form (G-actin). It was purified by polymerization to F-actin at room temperature with 0.01 M KCl, 60 minutes. The F-actin was pelleted by centrifugation at 65,000 g

for 3 1/2 hours. G-actin was then obtained by homogenizing the F-actin pellets in 0.2 mM ATP or εATP followed by another cycle of polymerization and centrifugation. The final purified G-actin was obtained by homogenizing the F-actin pellets in a medium containing 1 mM tris (hydroxymethyl) aminomethane (Tris) pH 8.0 and 0.2 mM ATP or εATP. The resulting solution was further purified by dialyzing against the same medium for 24 hours and clarified at 65,000 g for 3 1/2 hours. The actin prepared in this way was essentially free of contaminating tropomyosin as judged from viscosity measurements and from acrylamide gel electrophoresis in the presence of sodium dodecyl sulfate. Typically, the reduced viscosity for G-actin at a concentration of 2.0 mg/ml was 0.037 dl/g. The reduced viscosity of F-actin in this concentration range was 5 - 8 dl/g. The value of the reduced viscosity (0.037 dl/g) for G-actin at a concentration of 2.0 mg/ml is considered to be good evidence that the preparation is of high purity (Cohen, 1966). This value agrees well with the reduced viscosity of G-actin purified by Sephadex G-200 chromatography. In the early stage of this work, Sephadex G-200 chromatography was used to remove tropomyosin contamination (Rees and Young, 1967). It was subsequently found that, as the extraction technique was improved and carefully controlled, tropomyosin could be removed without gel filtration chromatography. The acrylamide gel patterns are shown in Figure 5. The right gel which was for an early preparation with a relatively high reduced viscosity shows a faint band immediately below the major band. This

FIGURE 5

Electrophoretic gel patterns of G-actin.

A 6 μg sample was applied to the acrylamide gel in the presence of sodium dodecyl sulfate. The right gel was for an early preparation and shows a band immediately below the major band. This second band indicates the presence of tropomyosin. The left gel was for a preparation without tropomyosin contamination.

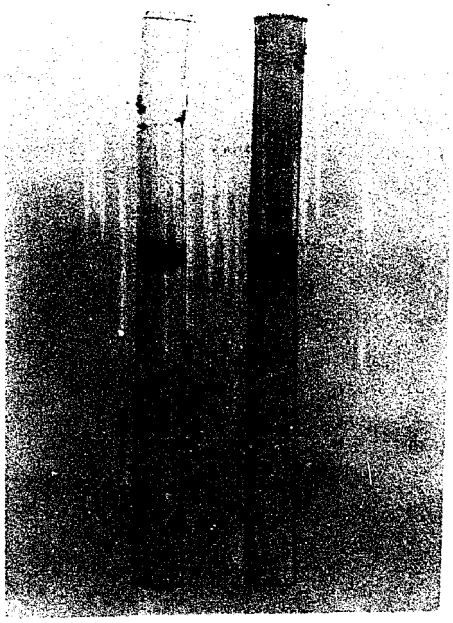

second band indicates the presence of tropomyosin (Bailin and Barany, 1972). The left gel was for a preparation which was judged to indicate the absence of tropomyosin contamination.

G-actin prepared in εATP and devoid of free εATP was prepared immediately prior to studies by treating G-actin (5 - 10 mg/ml) in 0.2 mM εATP at 0°C twice with 10% (v/v) Dowex 1-X2 (Asakura, 1961), each time for three minutes. The resin was immediately removed by centrifugation in a table top centrifuge. The supernatant was a complex of G-actin and εATP. The amount of εATP bound to this G-actin was estimated by heating the resin treated complex at 100°C (Martonosi, 1962) for two minutes followed by rapid cooling in cie water. The $MgCl_2$ concentration was then adjusted to 2 mM followed by heating again at 100°C for one minute and rapid cooling in ice water. The coagulated actin was removed from solution by centrifugation leaving the released nucleotide in the supernatant. The concentration of nucleotide in the supernatant was then determined by the absorbance at 275 nm. This procedure indicated that the resin treated actin was a 1:1 complex of εATP·G-actin (within 10%).

Myosin was prepared from rabbit skeletal muscle by a modified Szent-Gyorgyi method (Tomomura et al., 1966). Heavy meromyosin (HMM) was prepared from myosin dissolved in 0.6 M KCl by cleaving the myosin rod with 1 mg of trypsin (type I) per 250 mg of myosin. The trypsin treatment was carried out at room temperature for 10 minutes, and the reaction was stopped by 2 mg of soybean trypsin inhibitor. The heavy meromyosin fragment was separated from the

light meromyosin fragment by precipitating the latter in about 0.05 M KCl and the HMM fraction was subsequently purified with ammonium sulfate fractionations. The fraction precipitated between 40 and 60% saturation was HMM (Szent-Gyorgyi, 1953). It was dissolved in 0.6 M KCl, 1 mM Tris pH 8.0, and dialyzed against this same medium to remove excess ammonium sulfate. Complexes between F-actin and myosin or HMM (actomyosin or actomeromyosin) were prepared with freshly prepared samples of εADP·F-actin. Because of the large binding affinity of actin for HMM or myosin (binding constant of the order of 2×10^6 M^{-1}, Tonomura et al., 1966), an acto-HMM prepared by mixing 1.3 moles of HMM with an F-actin sample containing the equivalent of 1 mole of G-actin monomers can be regarded as a 1:1 complex. The 1:1 complex studied in this work was prepared in this way. Because of the denaturation of εATP·G-actin in solution devoid of free εATP, polymerization with 0.1 M KCl must be initiated immediately after resin treatment to remove the free εATP. The samples of the complexes between F-actin and myosin or HMM were used within 5 hours after they were prepared.

Myosin concentration was determined by the Lowry method (Lowry et al., 1951), and HMM concentration was determined from its absorbance at 280 nm, using an $E^{1\%}_{1cm} = 6.47$ (Harrington, 1964). Actin concentration was determined from its absorbance at 280 nm, using an $E^{1\%}_{1cm} = 10.97$ (Rees and Young, 1967).

Viscosity was measured with Cannon semi-micro viscometers having outflow times of around 30 seconds for water. The

viscometers were immersed in a constant temperature bath set at 25 ± 0.3°C.

Acrylamide gel electrophoresis was carried out on 10% gels as described by Weber and Osborn (1969), in the presence of 0.1% sodium dodecyl sulfate (SDS). The buffer system used was 50 mM phosphate at pH 8.0. Protein samples were incubated in the phosphate buffer containing 8 M urea, 1% β-mercaptoethanol and 1% SDS at 100°C for 2 minutes before they were applied to the gels.

C. Inactivation Studies

When G-actin is denatured either by heat or by removal of cations, it loses the ability to polymerize. The rate of inactivation was studied by measuring the loss of polymerizability. This loss was followed by measuring the decrease in viscosity of aliquots of G-actin that were polymerized at intervals (Asakura, 1961; West, 1970a). Prior to polymerization the sample of a 1:1 complex of εATP·G-actin was kept either in ice or maintained at 25°C in a constant temperature bath. At various time intervals, aliquots were removed and polymerized by adding 0.1 M KCl, 1 mM Mg^{++}, and 0.66 mM free nucleotide. Polymerization was allowed to proceed at room temperature for at least 60 minutes. For the effect of free nucleotides on inactivation, the free nucleotide was added at zero time and aliquots were subsequently polymerized at intervals. When EDTA was used as the inactivator, zero time

corresponded to the simultaneous addition of 1 mM EDTA to all samples.

D. Absorbance Measurements

Absorbance measurements were carried out in a Beckman Acta III spectrophotometer, equipped with an expanded scale, 0.0 - 0.1 absorbance unit full scale. Difference absorbance measurements were carried out with a pair of matched split cells. The optical path of each compartment of these cells was 4.5 mm. When the time course of actin polymerization was followed by the change in absorbance at 234 nm, the split cells were used. One compartment of both the reference and sample cells contained G-actin in 0.2 mM ATP (or εATP), 1 mM Tris, pH 8.0 of identical concentration. The other compartment of the reference cell contained 0.1 M KCl in the same solvent; the second compartment of the sample cell contained solvent only. At zero time, 0.1 M KCl was added to the actin compartment of the sample cell to initiate polymerization. The increase in absorbance at 234 nm was recorded on the 0.0 - 0.1 scale.

E. Fluoresence Studies

1. Steady State

Fluorescence excitation and emission spectra were measured in a ratio spectrofluorometer similar to one reported in the literature (Cheung and Morales, 1969). Spectra were obtained

using a rhodamine quantum counter (5×10^{-3} M in ethylene glycol) to correct for variation of the xenon lamp intensity with wavelength and to correct for fluctuation of the lamp intensity. The emission spectra are uncorrected for variation of the response of the detector system with wavelength. The excitation spectra reported here are the corrected spectra with an additional correction made for inner filter effect arising from high absorbance of the sample (Parker and Barnes, 1957).

The relative quantum efficiency, ϕ_S, was determined by a method described by Parker (1968):

$$\phi_S = \frac{A_S}{A_r} \cdot \frac{OD_r}{OD_S} \cdot \phi_r \qquad (1)$$

where A_r refers to the area of the corrected emission spectrum of a reference material, OD_r to the absorbance of the reference material at the excitation wavelength, and ϕ_r the quantum efficiency of the reference material; A_S refers to the area of the corrected emission spectrum of the sample; and OD_S to the absorbance of the sample at the excitation wavelength. Since the quantum efficiency for unbound εATP is known (Secrist et al., 1972b), it can be used as the reference material for the determination of the efficiency of εATP (ϕ_S) bound to actin. Since the spectral shape of both free and bound εATP is the same and since the emission maximum is identical for both species, it is not necessary to measure the areas from corrected emission spectra.

Steady state polarization measurements were carried out in the same ratio spectrofluorometer. Vertically polarized

monochromatic light from a Polaroid HNP'B film located in front of the sample cell was used for excitation. The polarized emission was isolated at right angles to the excitation direction by means of a pair of Corning 3-74 filters and a pair of Polaroid HNP'B films as analyzers. The analyzers were placed on both sides of the sample cell; one was oriented to pass radiation with electric vectors parallel to the electric vector of the exciting light ($I_{\parallel}$), and the other oriented at right angles to the first one for isolating the perpendicular component of the emitted light ($I_{\perp}$). These two signals were detected simultaneously by two RCS 1P28 phototubes. The outputs from these phototubes were fed into a ratio detector and read from a digital multimeter (Keithley-160) as a ratio of either $I_{\parallel}/I_{\perp}$ or $I_{\perp}/I_{\parallel}$. The ratio $u = I_{\parallel}/I_{\perp}$ is directly proportional to the degree of polarization, defined as

$$P = \frac{I_{\parallel} - I_{\perp}}{I_{\parallel} + I_{\perp}} = \frac{u - 1}{u + 1} \qquad (2)$$

With this experimental arrangement, the time course of polarization can be recorded continuously on a strip chart recorder. Ratio measurements also allow direct detection of small changes in polarization as a function of time.

2. Nanosecond Fluorometry

Fluorescence decay time and time-dependent fluorescence polarization were measured in a single photon counting instrument (Tao, 1969). A schematic diagram of this instrument is given in Figure 6. The lamp consists of a General Radio radiation line

FIGURE 6

Schematic diagram of nanosecond fluorometer.

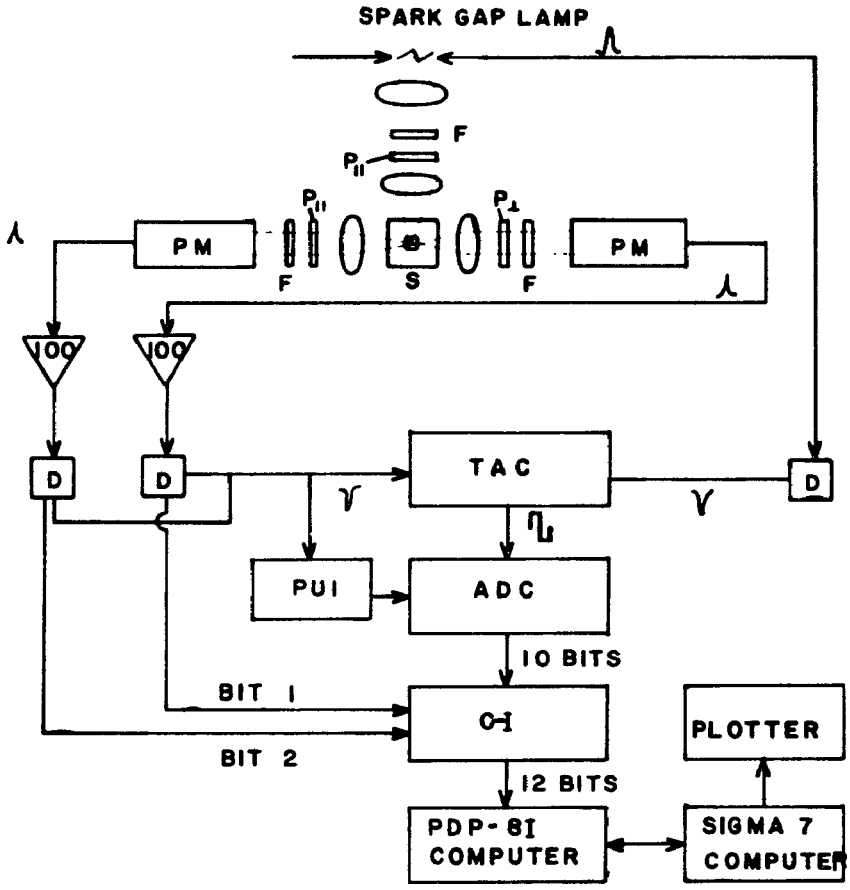

ADC	ANALOG TO DIGITAL CONVERTER
C I	COMPUTER INTERFACE
D	DISCRIMINATOR
F	FILTER
P	POLARIZER
PUI	PILE-UP INSPECTOR
PM	PHOTOMULTIPLIER TUBE
S	SAMPLE CHAMBER
TAC	TIME TO AMPLITUDE CONVERTER

NANOSECOND FLUOROMETER

modified to provide a spark gap in atmospheric air. The light pulses with a rise time of a few nanoseconds were used to excite the sample. The exciting light was isolated either with a Jarrell-Ash 0.25 meter grating monochromator or a narrow band pass filter. For polarization measurements, Polar coats were used as polarizer and analyzers with $I_{\parallel}(t)$ and $I_{\perp}(t)$ measured simultaneously by two Amperex 56 DUV photomultiplier tubes. A time-to-amplitude converter (TAC) was used to measure the time difference between an exciting light pulse and the detection of a photon in either photomultiplier. The output of the TAC was a signal whose amplitude was proportional to the time difference indicated above. The exciting intensity was attenuated so that less than 5 pulses were received at the input of the TAC from the photomultipliers for every 100 electrical lamp signals received at the TAC input. These conditions assured that not more than one photon was detected by the photomultiplier per exciting light pulse. If after these precautions multiple photons were still received, the pile-up inspector (PUI) discarded this set of data. The input of the TAC was then digitized by an analog-to-digital converter (ADC) to form 10 bits of a 12 bit computer word. The remaining bits were used to signify the photomultiplier from which the data originated. The data were collected in a PDP-8I computer and were plotted in a Cal-Comp plotter through a Sigma 7 computer. For lifetime studies, the data are plotted as the logarithm of the intensity (photon counts) against time, and for polarization studies, the data are plotted as the logarithm of the fluorescence anisotropy

against time, where the anisotropy, R(t), is given by

$$r(t) = \frac{I_{\parallel}(t) - I_{\perp}(t)}{I_{\parallel}(t) + 2I_{\perp}(t)} \qquad (3)$$

and is proportional to the degree of polarization defined under "Steady State" section.

Comparison with published values for quinine sulfate (Chen, 1974) indicated that the lifetime values measured by this instrument were good to within ± 0.5 nanosecond.

IV. RESULTS

A. Characterization of εATP·G-actin

Two criteria were used to ascertain that εATP can substitute for regular ATP as a co-factor. One is the ability of G-actin prepared in εATP to polymerize and the other is the ability of this actin to form actomyosin with myosin (or actomeromyosin with heavy meromyosin). The rate and extent of polymerization can be followed by either viscosity or optical measurements. The optical method is based on the observations made by Higashi and Oosawa (1965) that the absorbance of G-actin at 234 nm increased upon polymerization by addition of 0.1 M KCl. This increase was in parallel with increases in both viscosity and flow birefringence, and therefore can be used to follow polymerization. Using a pair of split cells the change in absorbance at 234 nm was recorded as a function of time after polymerization was started by adding 0.1 M KCl. The results are shown in Figure 7, along with the time dependence for a sample that was prepared with ATP. The initial rate of the polymerization as reflected by the increase in absorbance for G-actin prepared in εATP is essentially the same as that for G-actin prepared from ATP. The final extent of polymerization (i.e., the particle weight of the polymerized F-actin) is dependent upon the age of the G-actin sample as well

FIGURE 7

Polymerization rate of G-actin prepared in εATP and ATP.

Polymerization rate of G-actin prepared in εATP and ATP, 25°C, 1 mM Tris, pH 8.0. (____) G-actin in ATP. (----) G-actin in εATP. Actin concentration was 0.6 mg/ml in 0.2 mM ATP or εATP. Polymerization was initiated at zero time with 0.1 M KCl, and the time course was followed by recording the change in absorbance at 234 nm; optical path 0.4 cm.

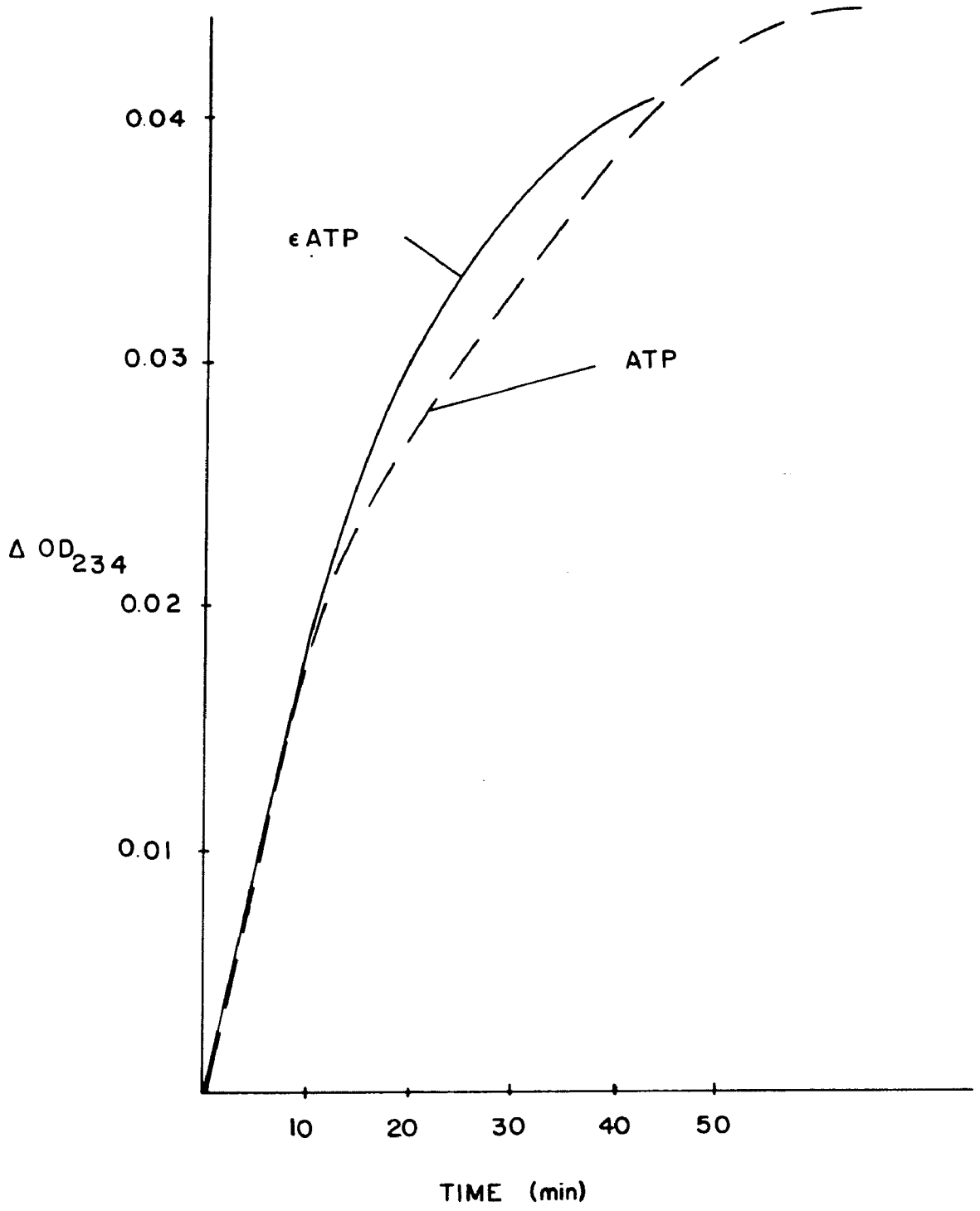
0.04
0.03
0.02
0.01
Δ OD234
εATP
ATP
10
20
30
40
50
TIME (min)

as the initial concentration. The reduced viscosity of the polymerized actin was in the range 5 - 8 dl/g, a value similar to that for actin polymerized in ATP.

Actin prepared in ATP forms a complex with either myosin or HMM. If the KCl concentration > 0.3 M this formation results in a large increase in viscosity. Pyrophosphate, ATP, or εATP dissociates this complex with a corresponding drop in viscosity. The same complex formation was demonstrated for εADP·F-actin, as shown in Figure 8. The viscosity of a mixture of εADP·F-actin and myosin (or HMM) at a molar ratio of 1:1.3 is several times higher than the sum of the viscosity values of the two individual components. This complex can be dissociated by εATP, as evidenced by the drop in viscosity after εATP addition. The gradual increase in viscosity subsequent to the initial drop is due to εATP hydrolysis. As εATP was depleted, the two species begin to recombine again, recovering most of the original viscosity of the complex. A second addition of εATP and the cycle can be repeated.

Another demonstration of complex formation was obtained from fluorescence polarization studies. Since the rotational relaxation time of a spherical macromolecule is given by $\rho = 3\eta V/RT$ (Tanford, 1961) where η is viscosity of the solvent, V is molecular volume, R is the gas constant, and T the absolute temperature, complex formation with another molecule should increase the relaxation time. As will be shown in another section, this relaxation time is proportional to the measured fluorescence polarization value. Therefore, the interaction between εADP·F-actin and HMM (or myosin) can be followed by measuring a polarization parameter (such as

FIGURE 8

Viscometric demonstration of complex formation between εADP·F-actin and myosin (AM) and εADP·F-actin and HMM (AH).

Actin concentration was 0.6 mg/ml, myosin concentration was 1.8 mg/ml, and HMM concentration was 0.7 mg/ml. All viscosity measurements were at 12.5 mM Tris, pH 8.0, 1 mM $MgCl_2$, 25°C, 0.6 M KCl. εATP was added at time indicated to give 1.67 mM εATP in the AM complex and 0.67 mM εATP in the AH complex.

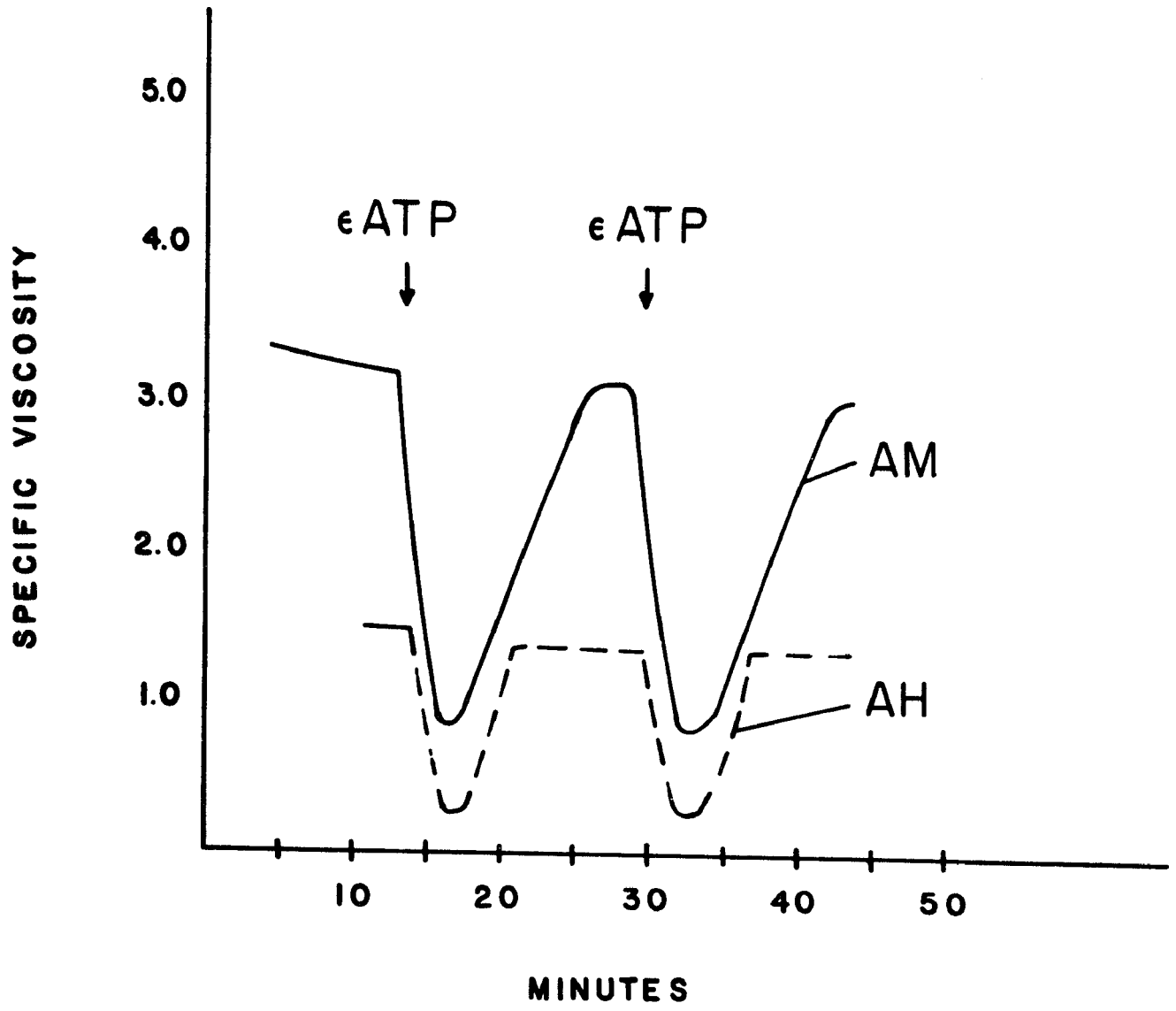
SPECIFIC VISCOSITY
5.0
4.0
3.0
2.0
1.0
εATP
εATP
AM
AH
10
20
30
40
50
MINUTES

$r = I_{\parallel}/I_{\perp}$) as a function of time. These results are shown in Figure 9. Addition of HMM to a solution of εADP·F-actin (1:1 complex, i.e. no free εADP) is accompanied by an increase in polarization as sensed by the bound nucleotide. This increase indicates complex formation. The addition of ATP dissociates the complex, thus reducing the extent of polarization. As ATP is depleted, recombination of the two proteins begins, thereby increasing the polarization parameter again. The cyclic change in polarization demonstrated here is equivalent to the cyclic change in viscosity, both indicative of a complex formation-dissociation cycle induced by ATP. ATP instead of εATP was used here to dissociate the εADP·F-actin-HMM complex because the presence of free εATP or εADP will also decrease the $I_{\parallel}/I_{\perp}$ ratio.

B. Binding of εATP to G-actin

Having now demonstrated that εATP can substitute for ATP as a co-factor for G-actin, the next set of experiments was designed to measure the binding affinity of the ATP analog for G-actin. As is known for ATP, the presence of added εATP protects the actin from denaturation, therefore, it is difficult to obtain stable G-actin devoid of bound nucleotide, and the conventional methods for binding studies, such as equilibrium dialysis, or titration with the ligand can not be directly used.

Asakura (1961) and later West (1970a) studied quantitatively the binding of nucleotide to G-actin in the presence of various

FIGURE 9

Demonstration by fluorescence polarization of complex formation between εADP·F-actin and HMM.

Actin concentration was 0.25 mg/ml, HMM concentration was 2.0 mg/ml. Measurements were made in 1 mM Tris, pH 8.0, 10°C, 0.6 M KCl. ATP was added at times indicated to give 1.2×10^{-5} M.

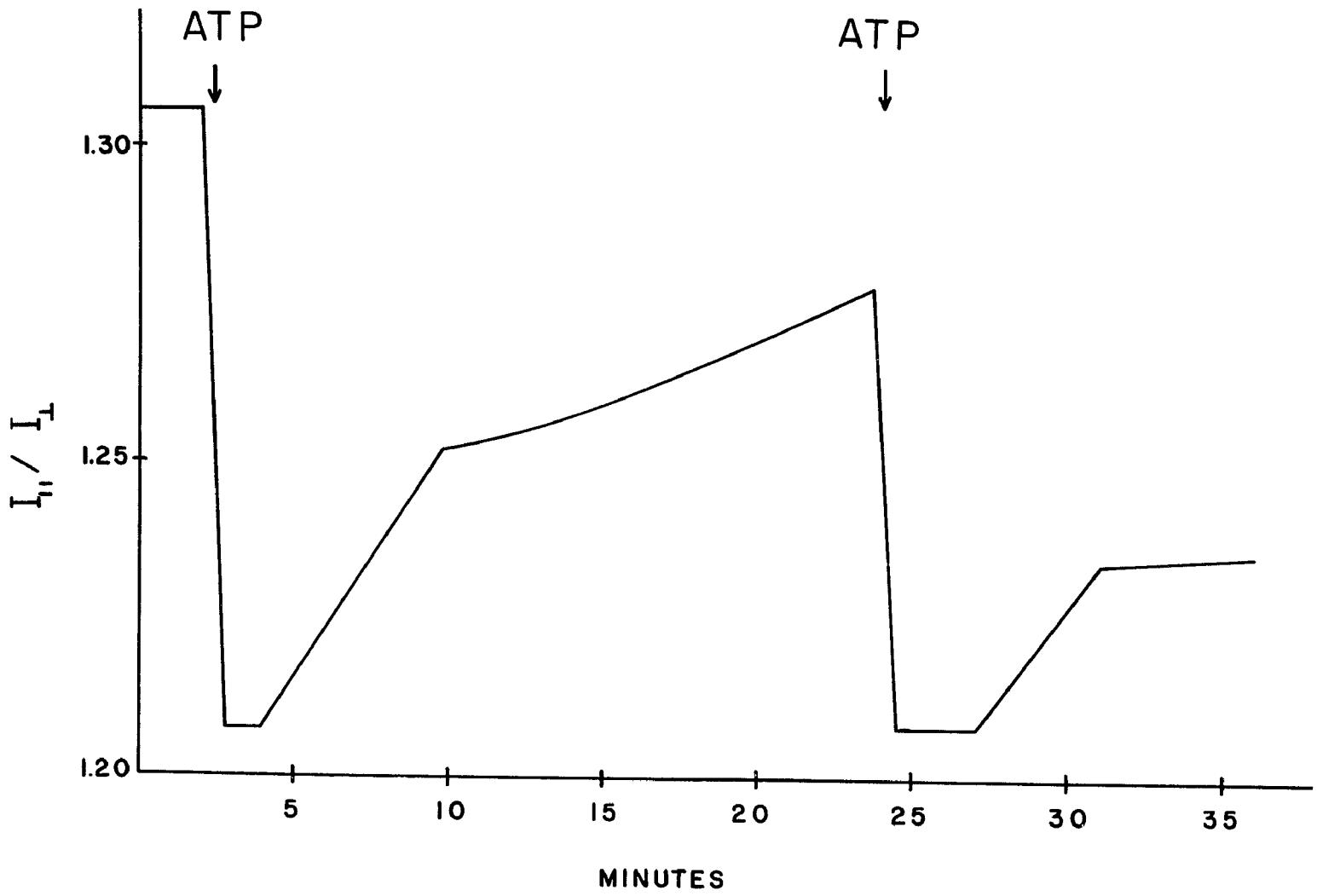
ATP
ATP
1.30
1.25
1.20
$I_{\parallel} / I_{\perp}$
5
10
15
20
25
30
35
MINUTES

concentrations of free nucleotide. After resin treatment to remove all free nucleotide, addition of various concentrations of nucleotide protected the actin from inactivation. The inactivation of actin can be described by the following equation:

$$\varepsilon ATP \cdot G \underset{\text{(a)}}{\rightleftharpoons} G \overset{\text{(b)}}{\rightarrow} I + \varepsilon ATP \qquad (4)$$

where εATP·G is the undissociated monomeric actin, G is the dissociated but not yet denatured form, I is the inactivated or denatured actin. Equilibrium reaction (a) occurs much faster than the irreversible reaction of step b and the concentration of G at any time is determined by equilibrium reaction (a) approximately independently of irreversible reaction (b) (Asakura, 1961). The analysis is restricted to the initial period of inactivation where the amount of inactive actin, I, can be neglected.

The dissociation constant for reaction (4) is

$$K_d = \frac{(G)\ (\varepsilon ATP)}{(\varepsilon ATP \cdot G)} \qquad (5)$$

Initially the rate of inactivation is

$$d(I)/dt = \alpha\ (G) \qquad (6)$$

When εATP is added to an actin solution devoid of free εATP, equation 5 becomes

$$K_d = \frac{(G)\ [(\varepsilon ATP)' + (G)]}{(\varepsilon ATP \cdot G)} \qquad (7)$$

where $(\varepsilon ATP)'$ is the concentration of added εATP. Let X_o be the initial molar concentration of εATP·G, and Z be defined as the

molar ratio of added εATP to initial εATP·G,

$$Z = \frac{(\varepsilon ATP)'}{(X_o)} \tag{8}$$

Equation 7 becomes

$$K_d = \frac{(G)\,[(X_o)Z + (G)]}{(X_o) - (G)} \tag{9}$$

Solving equation 9 for (G)

$$(G) = \frac{1}{2}\left(\left\{[(X_o)Z + K_d]^2 + 4K_d(X_o)\right\}^{\frac{1}{2}} - [(X_o)Z + K_d]\right) \tag{10}$$

and substituting this expression for (G) into equation (6),

$$\frac{dI}{dt} = \alpha\,(G) = \frac{\alpha}{2}\left(\left\{[(X_o)Z + K_d]^2 + 4K_d(X_o)\right\}^{\frac{1}{2}} - [(X_o)Z + K_d]\right) \tag{11}$$

Therefore, the binding constant of G-actin for εATP, $K_b = 1/K_d$, can be computed from a plot of the inactivation rate versus Z.

The inactivation data are shown in Figure 10 by plotting log (η_{rel}) versus time. Since it is the initial rate of inactivation that is sought, only the first few points are needed for calculating the rate. The rates are plotted as a function of $Z = (\varepsilon ATP)\cdot/(X_o)$ as shown in Figure 11. The curve is the computed best fit by a program designed to determine parameter values which give the best fit of the model to the data in the least squares sense. Viscometer run-out times are fed into the computer, from which viscosity (η_{rel}), and log (η_{rel}) are calculated with log (η_{rel}) being plotted versus time (Figure 10). The program then calculates initial rates and plots these against the parameter Z along with the computed best fit for these experimental points. The relative RMS error for the fitting procedure ranged from

FIGURE 10

Denaturation rates of εATP·G-actin.

7.5 mM Tris, pH 8.0, and 25°C. Effect of added εATP on inactivation rate: relative viscosity of εATP·G-actin polymerized at times indicated after addition of nucleotide. Actin concentration was 22 μM throughout. Concentration of added εATP (X μM): (●) 52.6, (X) 26.3, (○) 13.2, (◐) 6.6, and (□) 0.0.

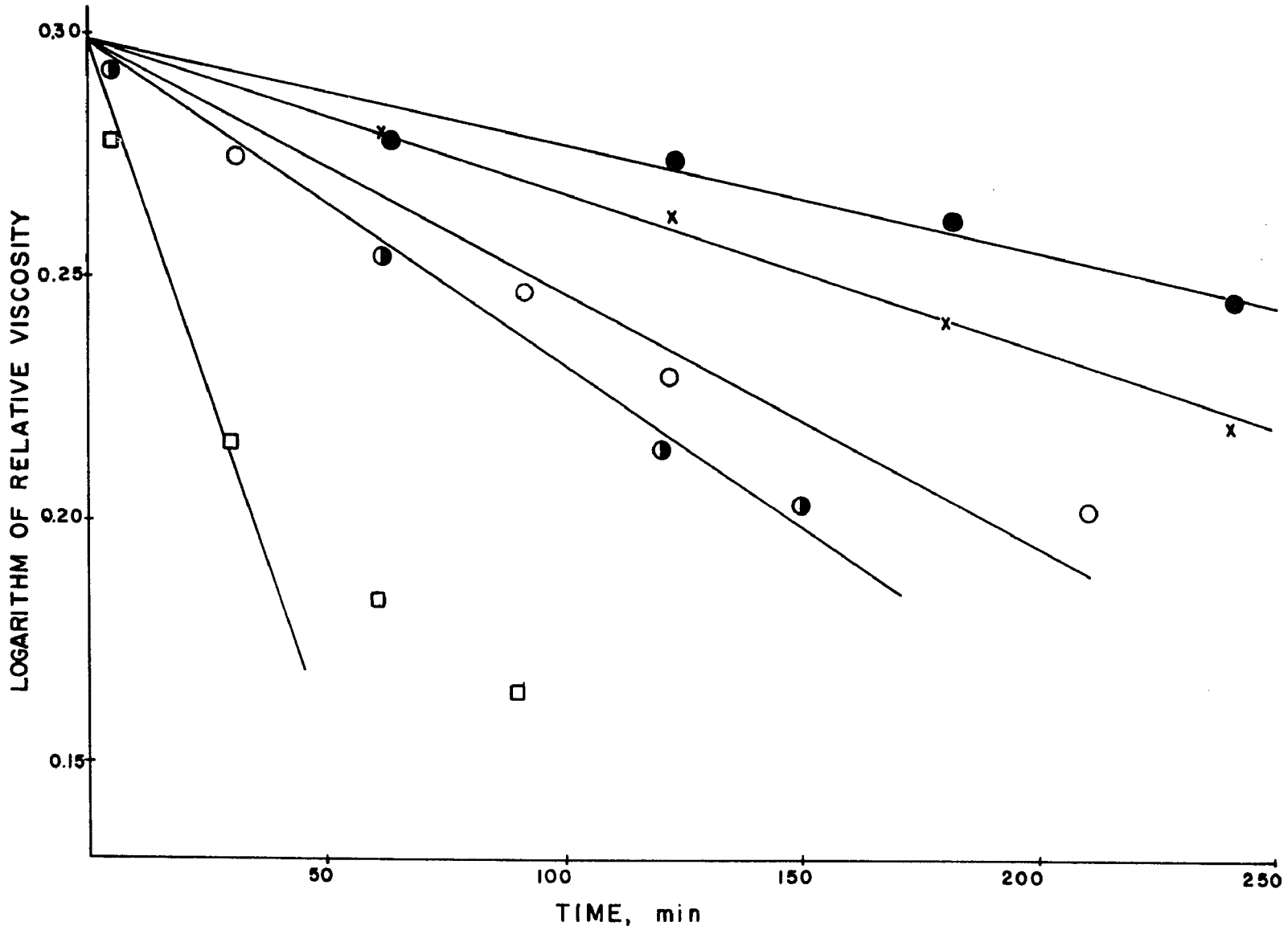
0.30
0.25
0.20
0.15
LOGARITHM OF RELATIVE VISCOSITY
50
100
150
200
250
TIME, min

FIGURE 11

Initial denaturation rates versus the parameter Z.

Initial rate of inactivation at various added εATP concentration are plotted against the Z parameter in equation 8. The curve is the computed best fit to the experimental points. Actin concentration and solvent conditions are the same as Figure 10.

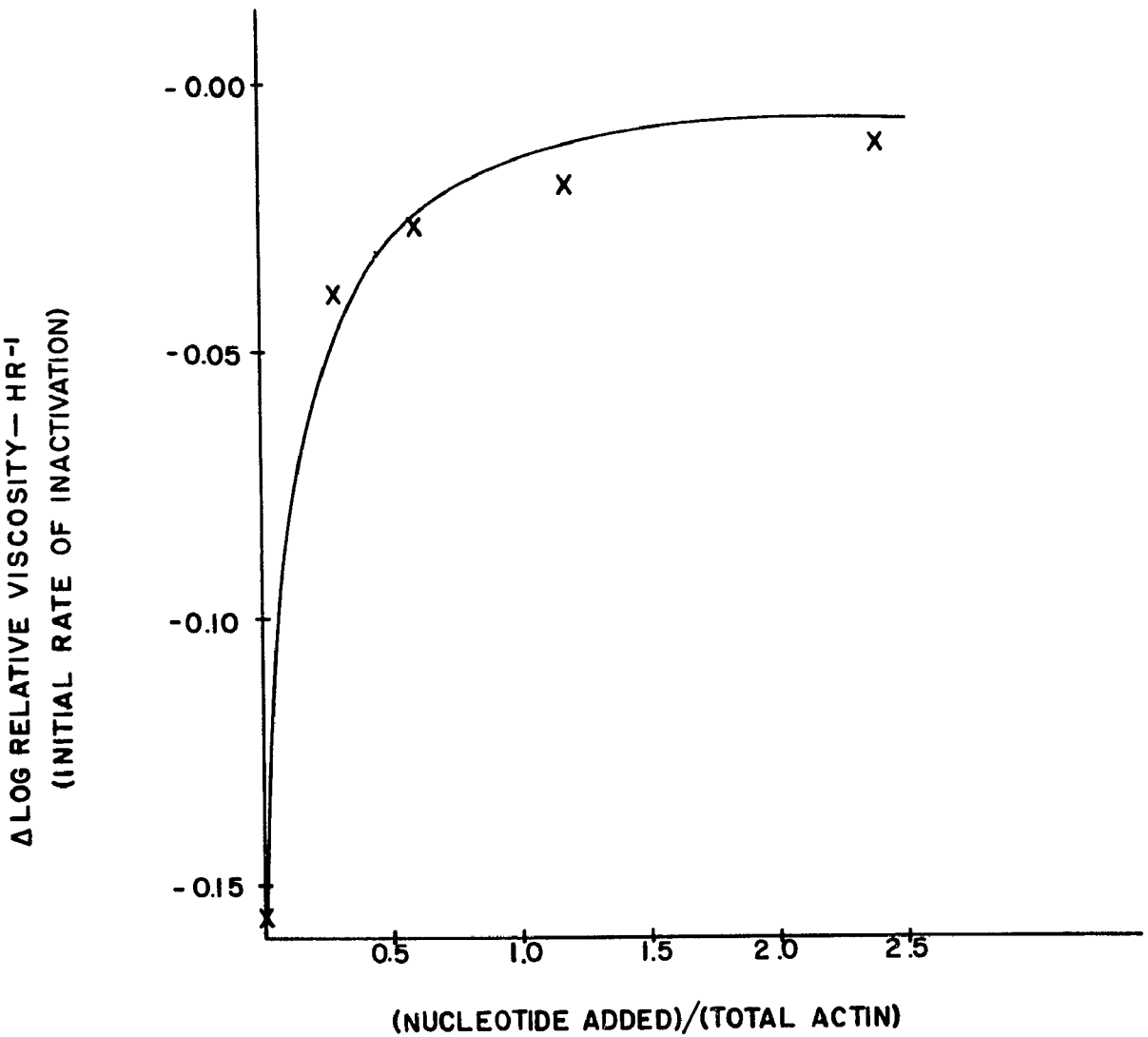
- 0.00
- 0.05
- 0.10
- 0.15
0.5
1.0
1.5
2.0
2.5
Δ LOG RELATIVE VISCOSITY — HR⁻¹
(INITIAL RATE OF INACTIVATION)
(NUCLEOTIDE ADDED)/(TOTAL ACTIN)

0.002 - 0.009 in the absence of EDTA and 0.05 - 0.09 in the presence of EDTA. The binding constants obtained from several actin preparations are listed in Table 1. In the absence of EDTA, the binding of G-actin for εATP ($4 - 5.7 \times 10^6$ M^{-1}) is about 50% of that for ATP. These values for εATP are about two orders of magnitude larger than that reported for ADP. In the presence of 1 mM EDTA, the binding constant is reduced to the range of $0.9 - 3.0 \times 10^5$ M^{-1}, as compared with the corresponding value of 3×10^5 M^{-1} for ATP and ADP (West, 1971).

C. Steady State Emission Properties of εATP·G-actin and εADP·F-actin

In all steady state emission measurements, the excitation wavelength was 310 nm. This wavelength corresponds to the shoulder of the absorption spectrum of εATP. Since actin and myosin (or HMM) have negligible absorbance at 310 nm, interference from intrinsic fluorescence of these proteins is minimized when the system is excited with 310 nm radiation.

Figure 12 shows that upon binding to G-actin (1:1 complex) in 1 mM Tris, pH 8.0, the emission of εATP remained near 415 nm with a decrease in relative quantum yield from 0.59 (Secrist et al., 1972b) to about 0.39 when excited at 310 nm. The polymerization of εATP·G-actin did not change the position of the emission peak, although there was a further decrease in quantum efficiency to 0.29.

TABLE I

Binding constants of ATP and εATP for G-actin

Nucleotide	Temp[a] (°C)	Binding Constant (M^{-1})
ATP	25	9.18×10^6
εATP	25	5.67×10^6
εATP	25	5.65×10^6
εATP	25	4.35×10^6
εATP + EDTA (1 mM)	0	1.50×10^5
εATP + EDTA (1 mM)	0	3.10×10^5
εATP + EDTA (1 mM)	0	0.93×10^5

(a) Temperature was controlled to ± 0.3°C.

FIGURE 12

Fluorescence emission spectra of εATP, εATP·G-actin (G) and εADP·F-actin (F).

Excitation was at 310 nm. Actin concentration was 0.25 mg/ml. All spectra were taken at 10°C, 1 mM Tris, pH 8. Concentration of the free εATP sample was 10^{-5} M.

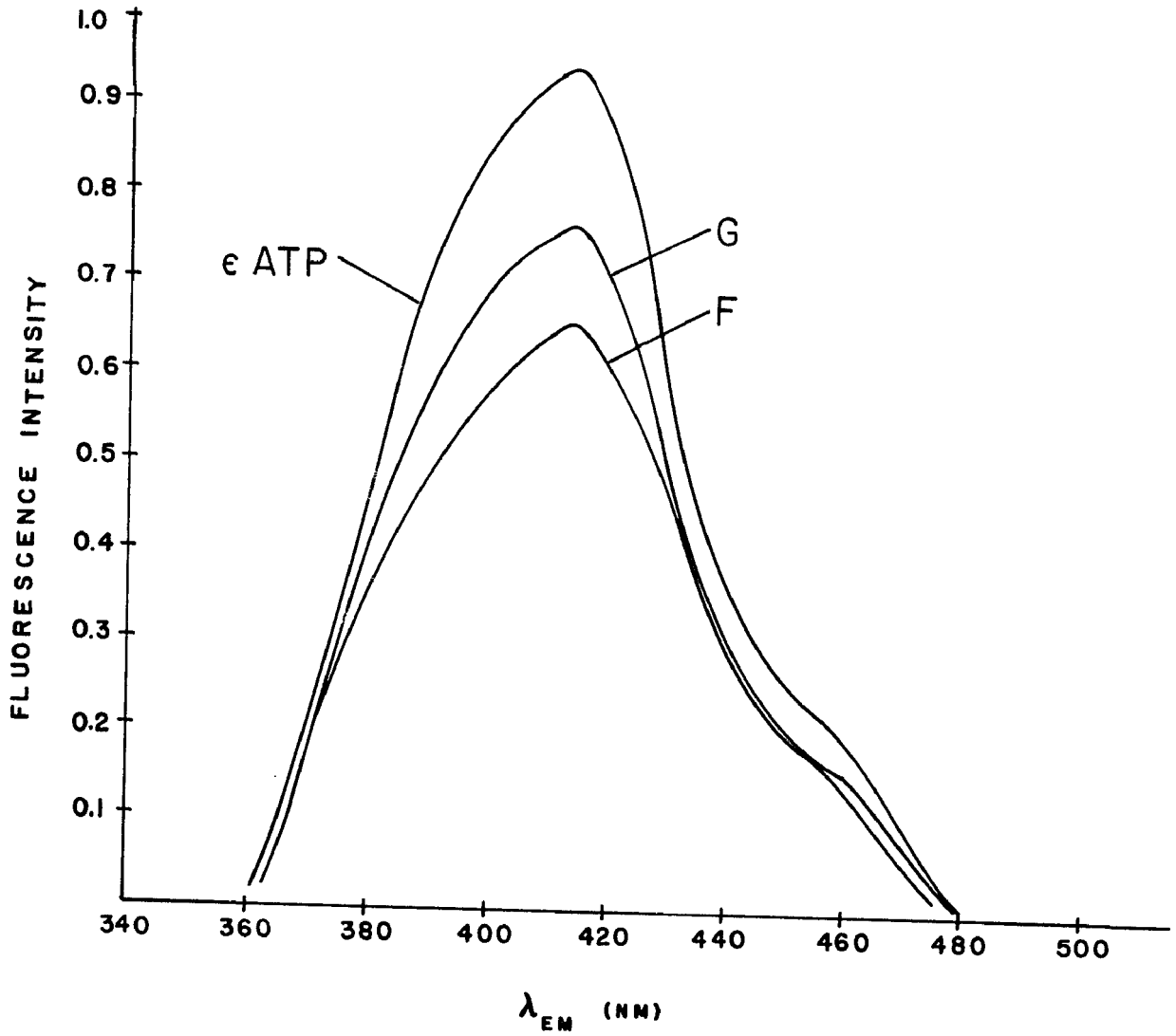
1.0
0.9
0.8
0.7
0.6
0.5
0.4
0.3
0.2
0.1
FLUORESCENCE INTENSITY
ε ATP
G
F
340
360
380
400
420
440
460
480
500
λEM (NM)

The fluorescence excitation spectrum of free εATP has two main peaks, one near 300, and the other at 275 nm (Figure 13). When bound to G-actin, the excitation spectrum showed a single peak near 280 nm, indicating transfer of excitation energy from protein chromophores to the bound nucleotide. Upon polymerization the excitation spectrum shows a decrease in this region indicative of a small decrease in energy transfer resulting from polymerization.

D. Nanosecond Emission Properties of εATP·G-actin and εADP·F-actin

When a molecule is excited to an upper electronic energy level, it may return to any of the rotational and vibrational levels of the original ground state either by fluorescence (emission of photons) or by internal conversion (non-radiative process), or it can change its electron pairing referred to as intersystem crossing. Fluorescence is the process of interest here. The excited state lifetime τ is related to the initial intensity (I_o) of the emitted light and the intensity at time t [I(t)] by

$$I(t) = I_o e^{-t/\tau} \qquad (12)$$

The lifetime, τ, is the time required for the intensity to drop to 1/e of its initial value, I_o.

Figure 14 shows semilogarithm plots of the fluorescent decay curves for free εATP, εATP·G-actin, and εADP·F-actin. These data

FIGURE 13

Fluorescence excitation spectra of εATP, εATP·G-actin (G), and εADP·F-actin (F).

Spectra taken at 10°C, 1 mM Tris, pH 8, with emission at 415 nm. Actin concentration was 0.25 mg/ml, and εATP concentration was 10^{-5} M. Fluorescence intensity was corrected for inner filter effect and variations in exciting light intensity.

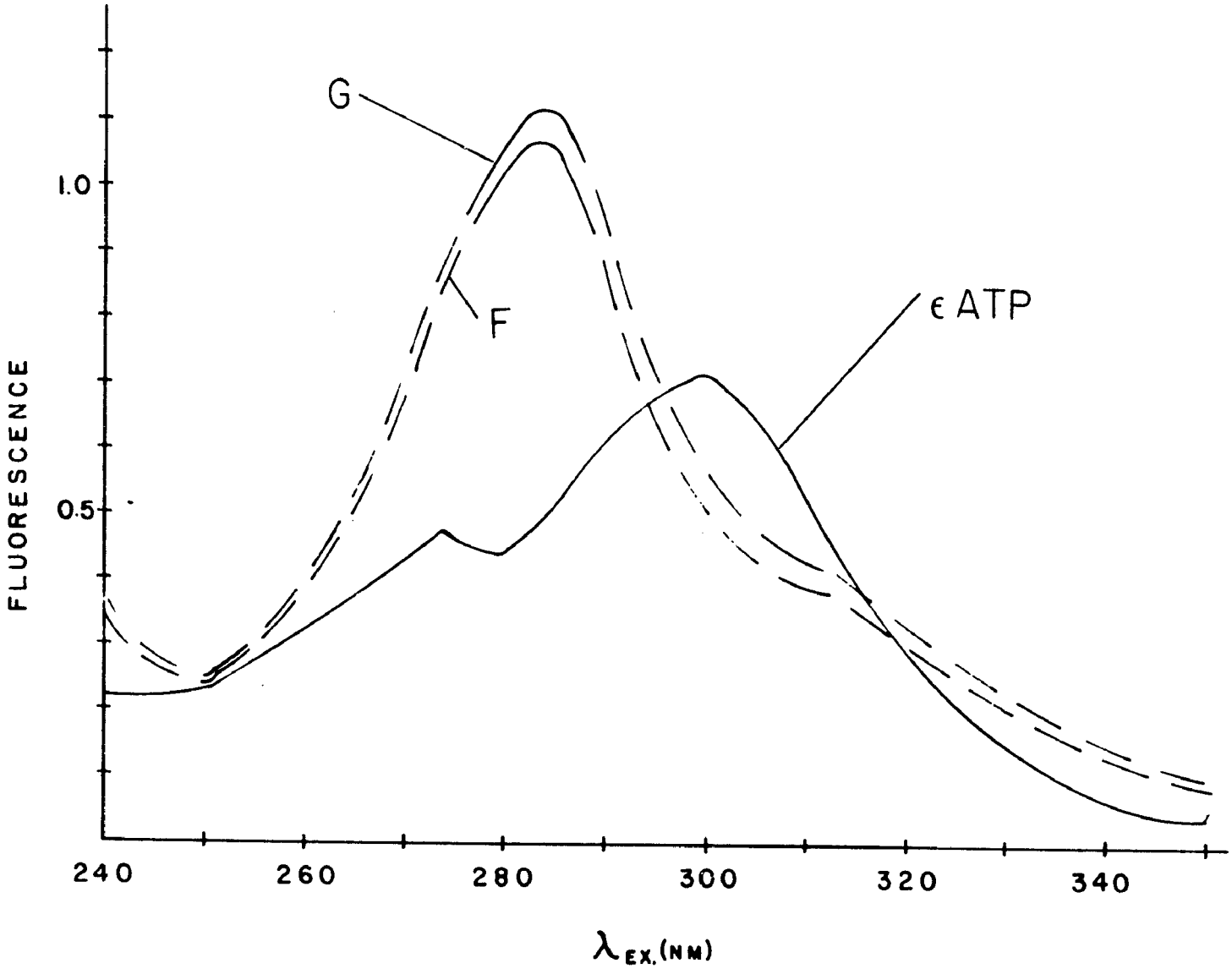
G
F
ε ATP
1.0
0.5
FLUORESCENCE
240
260
280
300
320
340
λ EX.(NM)

FIGURE 14

Fluorescence decay plots of εATP, εATP·G-actin (G), and εADP·F-actin (F).

Fluorescence intensity was measured in photon counts as a function of time. Excitation was at 310 nm. Actin concentration was 0.25 mg/ml, εATP sample concentration was 10^{-5} M. All spectra were taken at 10°C, 1 mM Tris, pH 8.0. KCl was added to the εADP·F-actin sample to a concentration of 0.6 M.

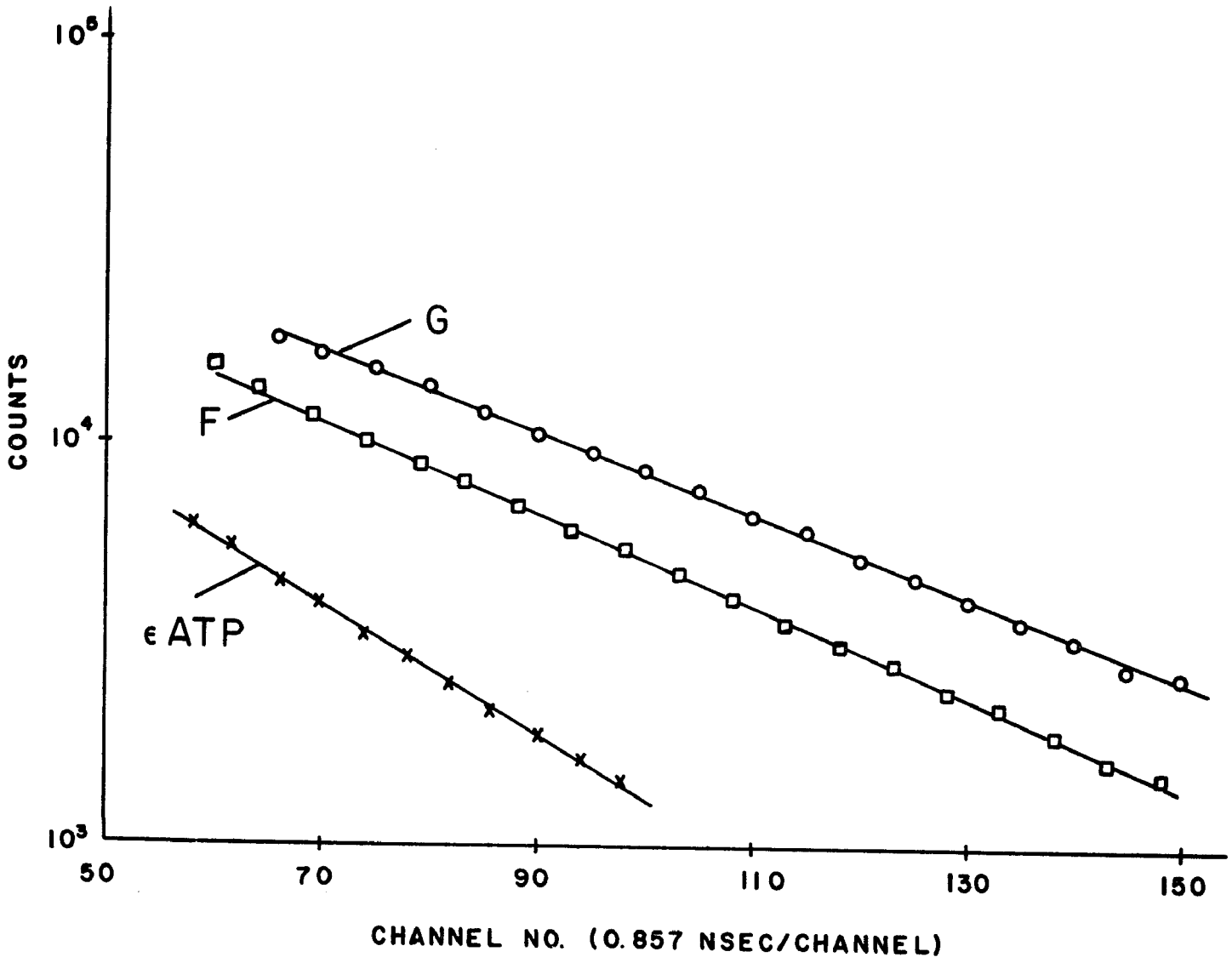
10^5
10^4
10^3
COUNTS
G
F
ϵ ATP
50
70
90
110
130
150
CHANNEL NO. (0.857 NSEC/CHANNEL)

were obtained by counting the number of emitted photons as a function of time immediately after excitation by a light pulse. The time is measured in channel number where one channel equals 0.857 nsec. These data points were analyzed by a single exponential function, from which the value of τ was computed. This procedure yielded the following values of τ: 26 ± 0.7 nsec. for εATP bound to G-actin; and 33 ± 0.6 nsec. for εADP bound to F-actin. The last value was obtained with a sample of F-actin which was polymerized from a 1:1 complex of εATP·G-actin.

E. Hydrodynamic Properties of G-actin and F-actin

Perrin (1926) has derived an equation relating the observed degree of fluorescence polarization, P, to the rotational relaxation time, ρ_o:

$$1/P - 1/3 = (1/P_o - 1/3)(1 + 3\tau/\rho_o) \qquad (13)$$

where P is observed polarization, P_o is the limiting polarization or polarization in the absence of Brownian motion, and τ is the excited state lifetime. Since $\rho_o = \frac{3\eta V}{RT}$, equation 13 can be rewritten as

$$1/P - 1/3 = (1/P_o - 1/3)(1 + RT\tau/\eta V) \qquad (14)$$

Comparison of equations 13 and 14 indicates that a plot of 1/P or (1/P - 1/3) against T/η should yield a straight line from which ρ_o can be readily calculated, provided τ is known. Weber (1952) has extended the Perrin equation to describe rigid ellipsoidal

macromolecules:

$$1/P - 1/3 = (1/P_o - 1/3)(1 + 3\tau/\rho_H) \qquad (15)$$

where ρ_H is the harmonic mean of the rotational relaxation times arising from rotations about the three principal axes of an ellipsoid of revolution. As is for the case of spherical molecules, a plot of 1/P or (1/P - 1/3) against T/η should give a straight line. From this plot, the value of ρ_H can be computed. It is to be noted that the magnitude of the three individual relaxation times cannot be obtained from this procedure.

The value of τ for εATP bound to G-actin has already been measured in this work (36.0 nsec.). The value of ρ_H can therefore be obtained from a Perrin-Weber plot according to equation 15, such as that shown in Figure 15. In these experiments, the polarization values were obtained from the measured ratio $I_\perp/I_{//}$ with a freshly prepared 1:1 complex of εATP and G-actin. The temperature of the sample was changed by increasing the temperature from about 4° to around 40°C. The value of ρ_H from this plot is 60.0 nsec. at 20°C, with a P_o value of 0.3. The polarization data for εADP·F-actin exhibited a zero slope when 1/P was plotted against T/η in the temperature range 4 - 30°C. These data show that the bound nucleotide does not sense any rotational mobility in F-actin in this temperature range, and therefore the relaxation time for F-actin cannot be obtained with such a probe. The limiting polarization, P_o, for F-actin was 0.19. The parameter P_o is defined as the limiting or intrinsic polarization of the molecule

FIGURE 15

Effect of temperature on the steady state fluorescence polarization of εATP·G-actin.

Buffer was 7.5 mM Tris, pH 8.0. The temperature was varied from 4° to 40°C. Actin concentration was 0.5 mg/ml.

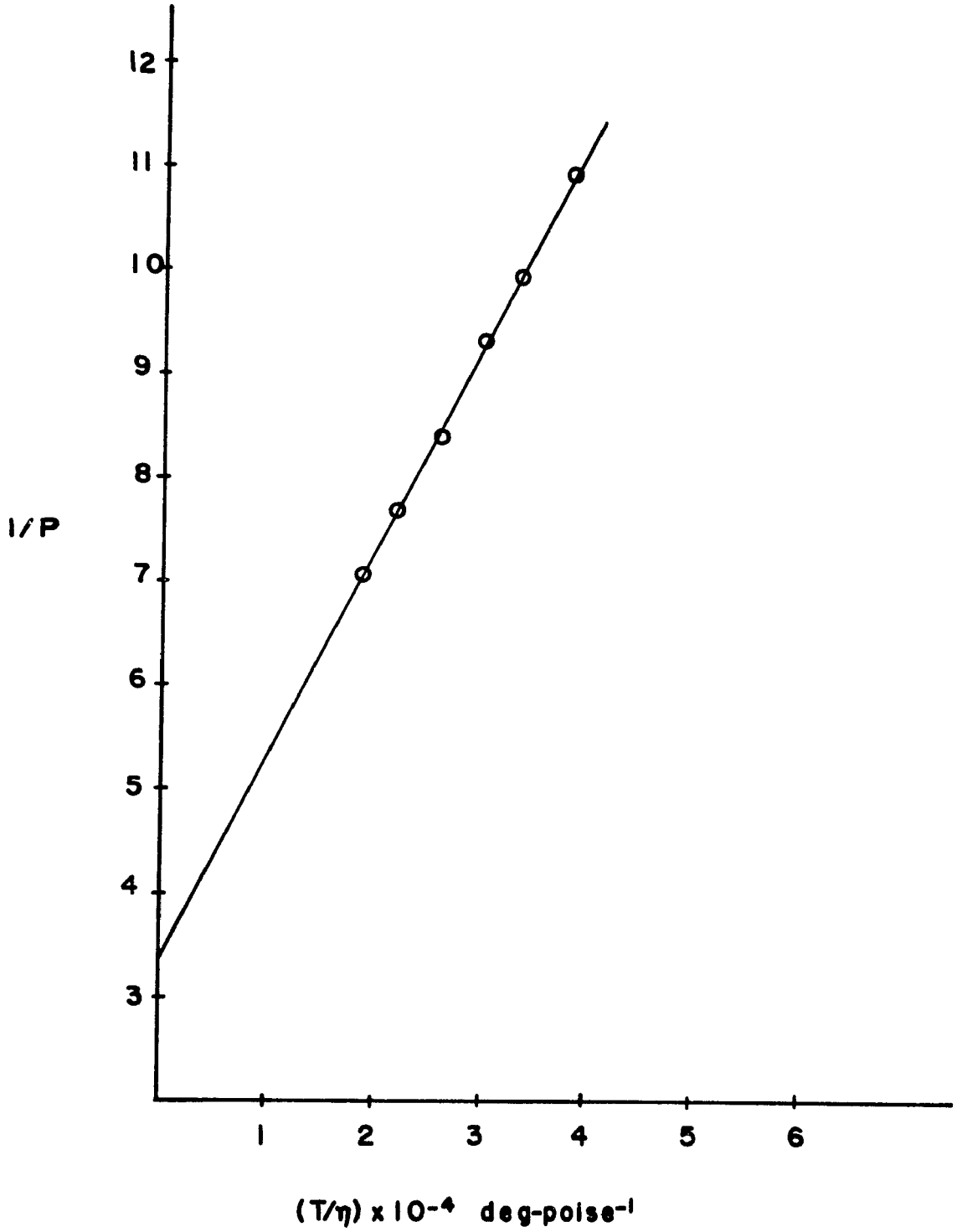
12
11
10
9
8
7
6
5
4
3
1/P
1
2
3
4
5
6
(T/η) x 10⁻⁴ deg-poise⁻¹

in the absence of any depolarization due to Brownian motion ($T/\eta = 0$). It is a function of the polarization due to absorption of light, the intramolecular angle of transfer between the absorption and emission dipoles, and the migration of excitation energy among bound nucleotide (Pesce et al., 1971).

The steady state polarization technique for obtaining rotational relaxation time involves the change of either temperature or viscosity by adding substances such as sucrose or glycerol. This can often result in complications such as thermal activation of the fluorophore, or denaturation of the protein. This can be circumvented by using the nanosecond technique (Stryer, 1968).

The time dependent anisotropy is defined as

$$r(t) = \frac{I_{\parallel}(t) - I_{\perp}(t)}{I_{\parallel}(t) + 2I_{\perp}(t)} \qquad (16)$$

where $I_{\parallel}$ and $I_{\perp}$ are now functions of time, t. The functional form of the anisotropy for a spherical molecule is given by Yguerabide et al. (1970)

$$r(t) = r_o e^{-t/\phi_o} \qquad (17)$$

where r_o is the anisotropy at the instant of excitation and is a function of the average angle between the absorption and emission oscillators of the molecule, t is time, and ϕ_o is the rotational correlation time and is related to the rotational relaxation time by

$$\phi_o = \rho_o/3 \qquad (18)$$

It can be seen that a semilogarithmic plot of r(t) versus time will allow the determination of ϕ (and hence ρ_o). This can be accomplished at a single temperature. The functional form of r(t) for non-spherical molecules is more complicated (as will be explained later under Discussion), but the individual correlation times can, in principle, be resolved from a single experiment carried out at one temperature.

Figure 16 shows the anisotropy decay curves of εATP·G-actin and εADP·F-actin. The plot for εADP·F-actin is essentially horizontal with a very large unmeasurable rotational correlation time. This, of course, is expected since the steady state polarization measurements already indicated that εADP is not suitable for determining the relaxation of F-actin. The correlation time for εATP·G-actin was about 26.0 nsec., corresponding to a relaxation time of 78.0 nsec.

F. Interaction of εADP·F-actin with Heavy Meromyosin

The complexing of εADP·F-actin with myosin and HMM is accompanied by a large increase in viscosity. On addition of εATP to the complex, the viscosity drops rapidly to a value equal to the sum of the individual viscosities of εADP·F-actin and myosin or HMM as shown in Figure 8. The viscosity increases as the added nucleotide is hydrolyzed. This cyclic response of viscosity to addition of εATP demonstrates for the first time the complex formation of εADP·F-actin with myosin and HMM.

FIGURE 16

Time dependent fluorescence nanosecond anisotropy of εADP·F-actin (F), and εATP·G-actin (G) as a function of time.

Excitation was at 310 nm. Actin concentration was 0.25 mg/ml. All spectra were taken at 10°C, 1 mM Tris, pH 8.0. KCl was added to the εADP·F-actin sample to a concentration of 0.1 M.

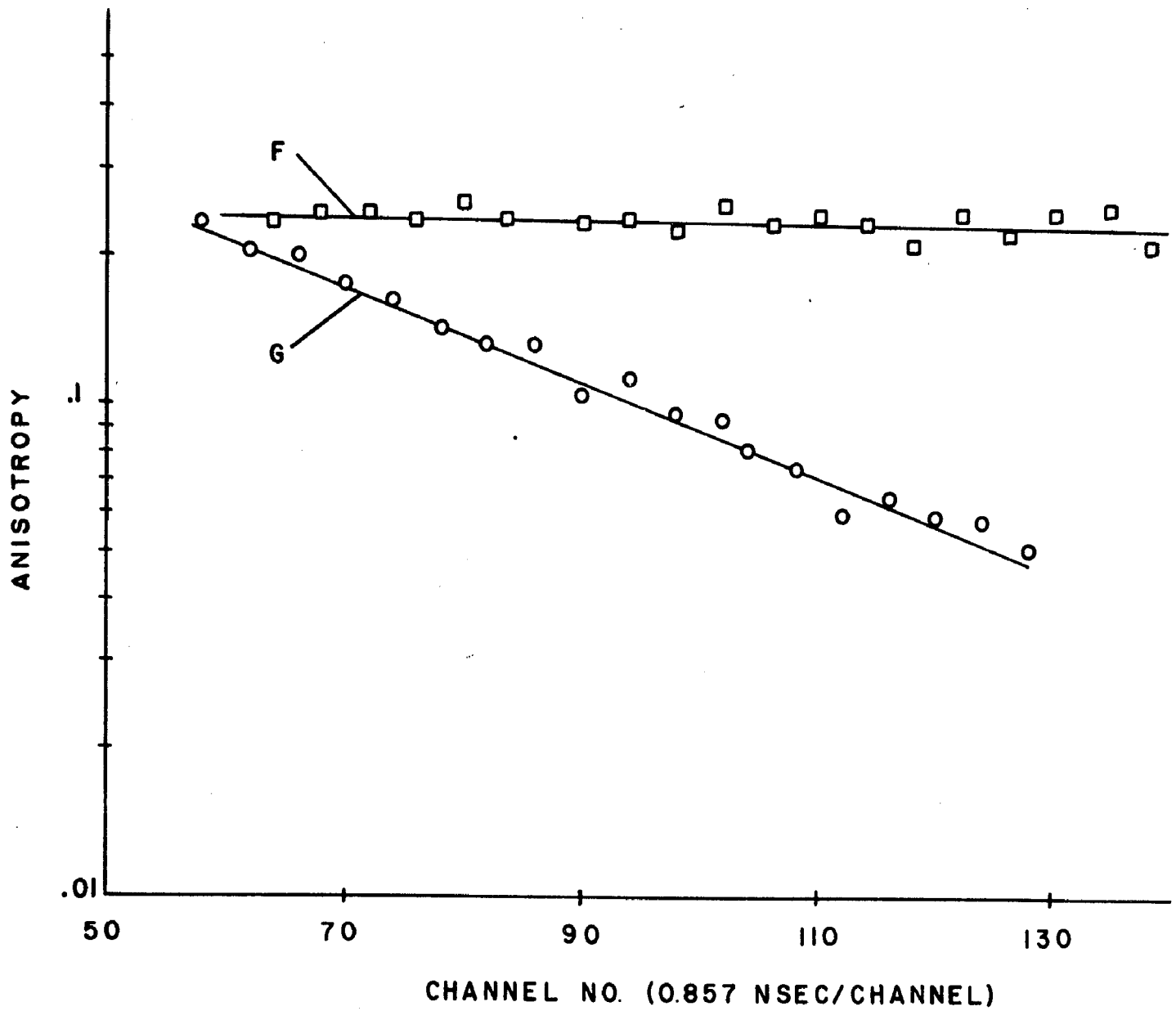
F
G
ANISOTROPY
.1
.01
50
70
90
110
130
CHANNEL NO. (0.857 NSEC/CHANNEL)

Figure 9 shows that the complex formation between εADP·F-actin and HMM can likewise be demonstrated by monitoring a parameter such as fluorescence polarization or the ratio of the parallel and perpendicular components of fluorescence as a function of time after addition of ATP. As with viscosity, on addition of ATP there is a rapid dissociation of the complex, as reflected by a drop in the polarization parameter, followed by an interval of a few minutes before recomplexing begins.

Figure 17 shows the emission spectra of εADP·F-actin, and the complex of εADP·F-actin and HMM. With the complex, increase in intrinsic emission in the 340 nm region is due to the presence of HMM. The dip in the nucleotide emission peak around 405 nm can be removed by the addition of pyrophosphate (PPi) to dissociate the complex. This observation and measurements carried out with εADP·F-actin in the presence of an added light scattering agent (ludox) indicate that the dip near 405 nm arises from light scattering which was caused by the large actomeromyosin complex.

Free εATP in solution has a lifetime of 26.0 nsec. (Table II). On binding to G-actin, the lifetime increases to 36.0 nsec. Polymerization of this G-actin to F-actin yields a lower lifetime of 33.0 nsec. The interaction of εADP·G-actin with HMM leads to a reduction of the lifetime of the bound nucleotide. At a molar ratio of 6:1 (actin : HMM), the lifetime is 30.5 nsec., and at a 1:1 ratio the lifetime further decreases to 29.2 nsec.

Figure 18 shows that the fluorescence anisotropy of εADP·F-actin in 0.6 M KCl had a small slope. When complexed with

FIGURE 17

Fluorescence emission spectra of εADP·F-actin (F), complex of εADP·F-actin and HMM (A/H), and the complex of εADP·F-actin and HMM plus pyrophosphate (A/H + PPi).

Excitation was at 310 nm. Actin concentration was 0.25 mg/ml (5.43×10^{-6} M), HMM concentration was 7.05×10^{-6} M. All spectra were taken at 10°C, 1 mM Tris, pH 8.0, 0.6 M KCl.

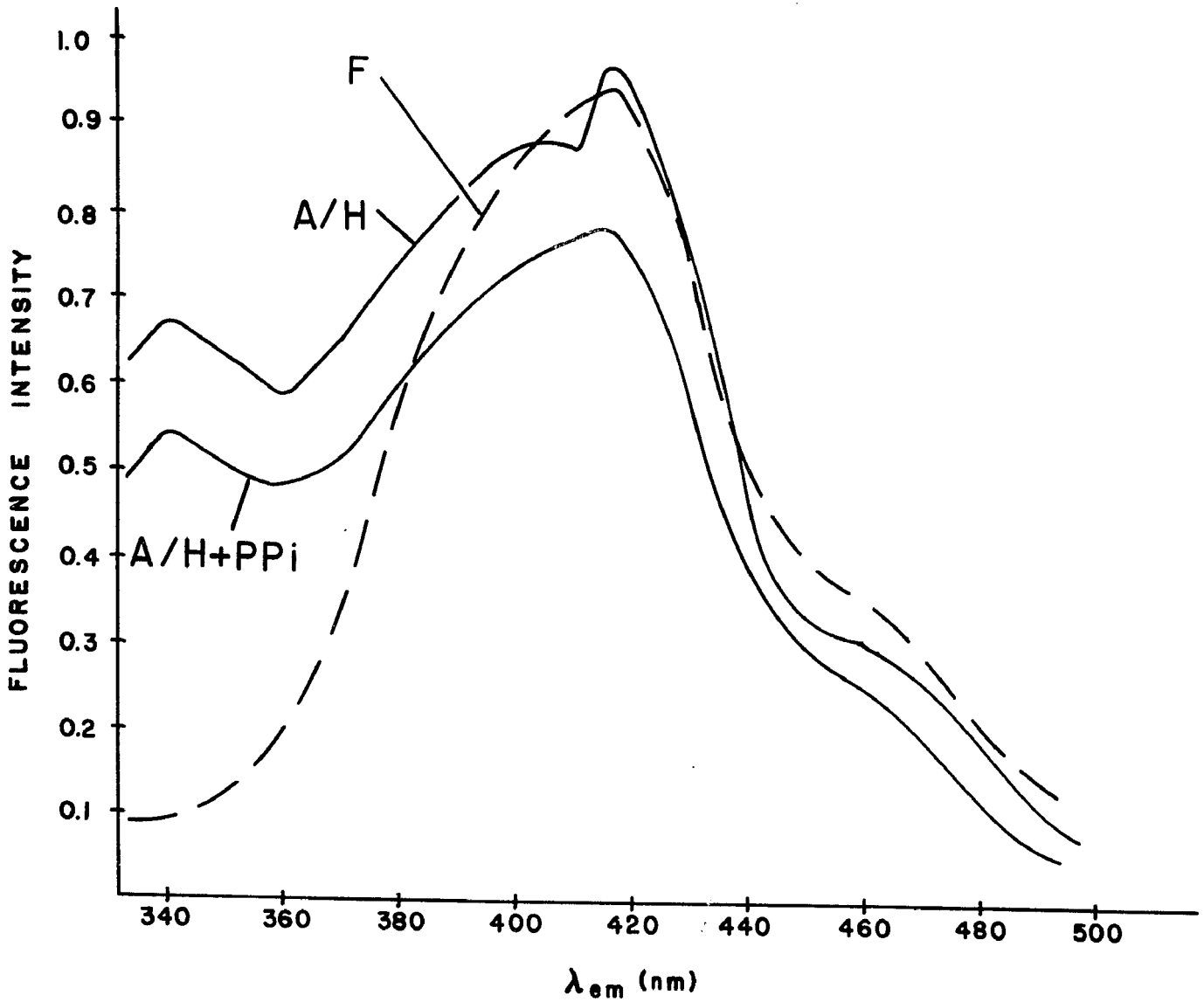
F
A/H
A/H+PPi
FLUORESCENCE INTENSITY
1.0
0.9
0.8
0.7
0.6
0.5
0.4
0.3
0.2
0.1
340
360
380
400
420
440
460
480
500
λem (nm)

TABLE II

Fluorescent lifetimes of actin bound nucleotide analogs

Fluorescent species	Lifetime (nsec.)
εATP	26.0 ± 1.0
εATP·G-actin	36.0 ± 0.7
εADP·F-actin	33.0 ± 0.6
εADP·F-acto HMM (1:1 complex)	29.2 ± 0.2
εADP·F-acto HMM (6:1 complex)	30.5 ± 0.5

FIGURE 18

Time dependence of the fluorescence nanosecond anisotropy of εADP·F-actin (F), and complexes of εADP·F-actin and HMM in molar ratios 1:1.3 (A/H 1/1.3), and 6:1 (A/H 6/1).

Excitation was at 310 nm. Actin concentration was 0.25 mg/ml (5.43×10^{-6} M). All spectra were taken at 10°C, 1 mM Tris, pH 8.0, 0.6 M KCl.

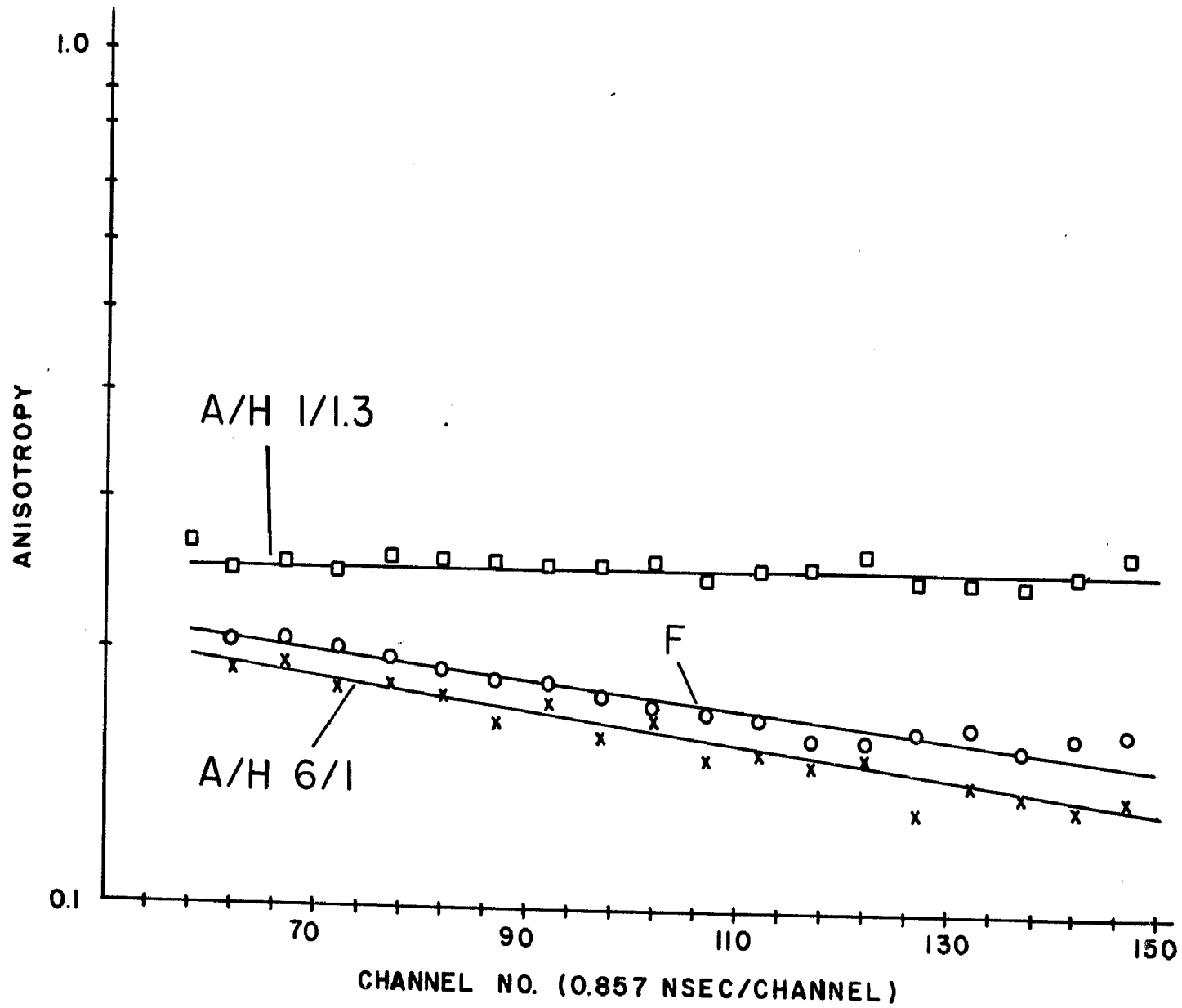
1.0
0.1
ANISOTROPY
A/H 1/1.3
F
A/H 6/1
70
90
110
130
150
CHANNEL NO. (0.857 NSEC/CHANNEL)

HMM in a molar ratio of 1 actin to 1.3 HMM, the anisotropy plot was flat indicating the formation of a large "rigid" complex. A complex of F-actin and HMM in a molar ratio of 6 actin to 1 HMM had a greater slope than εADP·F-actin alone. The correlation time for this 6:1 complex (200 nsec.) was 15% lower than that for F-actin alone (230 nsec.), suggesting that at this molar ratio, the bound HMM is imparting "flexibility" to the F-actin polymer.

V. DISCUSSION

A. Properties of εATP·G-actin and εADP·F-actin

The observation that εATP·G-actin polymerizes with a rate similar to ATP·G-actin and that εADP·F-actin complexes with HMM in 0.6 M KCl demonstrates the usefulness of this ATP analog in substituting for ATP on actin. Since the εATP can be excited with light of wavelength away from the protein absorption band with a resulting intense emission again away from the protein emission enables the ATP analog to serve as an optical probe for actin behavior.

In the absence or presence of EDTA, the binding of G-actin for εATP is about 50% of that for ATP. The weaker binding with this analog could be due to the masking of 1-N and 6-NH_2 in the adenine moiety. This reduced binding affinity, however, does not affect the polymerization process. The binding constants were obtained from measurements of the inactivation of G-actin nucleotide. For the data presented here viscosity measurements served as a measure of the inactivation rate in equation 11. Other possible methods for following the time dependence of inactivation are absorbance and fluorescence measurements, provided that denaturation is accompanied by such spectral changes. Absorbance measurement was ruled out in this work because the change in absorption was too

small to measure. Fluorescence polarization was explored. This was carried out by following the fluorescence polarization (or $I_\parallel / I_\perp$) as a function of time in the presence of various concentrations of excess εATP. As the G-actin denatures, εATP is released. The presence of this released nucleotide will decrease the total polarization. Thus a continuous recording of the decrease in polarization as a function of time will give the initial inactivation rate. Although the binding constant was not determined by this independent method, such a procedure was found to be feasible.

B. Emission Properties of Bound ε-Nucleotides

The emission curves for actin-bound εATP showed no shift in the emission maximum relative to free εATP in solution. This insensitivity of the emission maximum towards binding sites on proteins and toward polarity of environment has been observed by Miki et al. (1974) and Secrist et al. (1972b). There was a decrease in quantum yield of εATP on binding to G-actin. This decrease in fluorescence yield was accompanied by an increase of over 30% in lifetime. These data are discussed below by considering the fate of an excited electron.

When light of appropriate wavelength is absorbed by a molecule, the upper electronic singlet excited state is reached very rapidly so that no molecular motion either in the chromophore (Franck-Condon principle) or in its solvent environment can occur.

The only change taking place is that in the dipole moment of the chromophore and in its solvation shell. During the lifetime of the excited state several processes may take place:

1. The first involves the reorientation of solvent molecules around the new dipole. This will result in a stabilization of the excited state. In a more polar solvent, interaction between the excited state dipoles and solvent molecules results in the emission of a photon of low energy (Stryer, 1968). This interaction thus lowers the energy level of the equilibrium excited state from which the observed emission originates. This loss in energy resulting from the dipolar interaction shows up in the emission spectra as a shift in the wavelength of maximum emission to longer wavelengths. In nonpolar solvents, the dipolar interaction is either small or negligible and the corresponding loss in energy is small. Consequently, the emission maximum of the same chromophore in a nonpolar solvent is blue-shifted relative to that in a polar solvent. It is this type of excited state interaction which allows investigation of micropolarity on protein binding sites with fluorescent probes. $1,N^6$-ethenoadenosine triphosphate, however, senses no polarity effects on binding to G-actin, nor does εADP bound to F-actin

when the latter complexes with HMM. This lack of spectral shift cannot be taken to indicate similar micropolarity, as has been pointed out by Secrist et al. (1972b). With the majority of solvent systems, changes in quantum yield occur in parallel with changes in emission maximum. However, there are exceptions to the correlation between emission maximum and quantum yield, suggesting that specific quenching mechanisms may be important.

2. A second process that can occur during the excited state lifetime is a change in geometry of the chromophore. This may arise either because of a change in force constant or in bond length or both in the excited state. If this change results in a small overlap between the absorption and emission bands, then the quantum yield of fluorescence will be small (Radda, 1972). If the geometrical change is in the opposite direction leading to a large emission overlap, a large fluorescent quantum yield will be expected.

3. There are several quenching processes which can affect the quantum yield. Some fluorescent molecules can be quenched immediately upon excitation due to their close proximity to

quencher molecules predating excitation. This is known as static quenching (Boaz and Rollefson, 1950), which takes place before excitation has occurred and is a consequence of the reduction of the number of fluorophore molecules available for excitation. This reduction, for example, can result from complex formation with neighboring molecular species. Thus, static quenching is reflected in the measured quantum yields. One such possible process is proton transfer (Spencer et al., 1974). Since the time course of static quenching is much shorter than the excited state lifetime, it will not show up in the measured lifetimes. Other excited molecules can be quenched by time-dependent processes (dynamic quenching) occurring during the lifetime of the excited state. This type of quenching results from depopulation of the excited state and will be reflected in both quantum yields and lifetime.

4. Transfer of excitation energy through a resonance mechanism to a second chromophore with appropriate spectroscopic properties will also result in fluorescence quenching in donor and an enhancement in the acceptor molecule. In this case, the transfer leads

to a decrease in both lifetime and quantum yield. This is the usual mechanism for sensitized emission (Pesce et al., 1971).

5. There is a low probability that the excited electron will change its spin. When this occurs, the molecule is then said to be in a triplet excited state. This conversion from the singlet excited state to the triplet excited state is termed intersystem crossing, and transition from the triplet to the ground state (phosphorescence) may occur by mechanisms similar to those for the singlet state. The triplet state is characterized by longer excited state lifetimes (10^{-3} to several seconds or even longer) which increase its susceptibility to quenching mechanisms (Pesce et al., 1971).

Of the 5 processes discussed above, intersystem crossing to the triplet state and transfer of excitation energy can be ruled out immediately as possible causes for the observed emission properties for bound εATP and εADP. This follows from the facts that (1) the increased lifetimes when these nucleotides are bound are still several orders of magnitude smaller than that for phosphorescence, (2) changes in fluorescence yield and lifetime are in opposite directions, and (3) no potential energy acceptor is present in the εATP·G-actin complex (a potential acceptor from εATP must be one whose absorption band overlaps the emission band of εATP. In other

words, this acceptor chromophore must possess an absorption spectrum in the visible region and such a chromophore does not exist.

The fact that the fluorescence yield and lifetime change in opposite direction suggests that more than one process is involved leading to the observed emission properties. The decrease in quantum yield of εATP on binding to G-actin could be due to its binding at a site in close proximity to a tryptophane or tyrosin residue. These residues could donate a proton to the bound nucleotide, forming a statically quenched dark complex. Spencer et al. (1974) have shown that it is the neutral species of εAMP that is responsible for its emission. Protonation of the most basic nitrogen at the 9-position of the adenine moiety (Figure 4) decreased the quantum yield. This protonation results in static quenching, a process which can be picked up only by steady state measurements (quantum yield) and not by dynamic measurements (lifetime). Thus, at pH values below the pK (around 3.9), the values of quantum yield decreased systematically while lifetime values remained essentially unchanged. West (1970b) using difference absorption has suggested that tyrosine and tryptophane are located near the nucleotide binding site on actin. That the bound nucleotide in G-actin may interact with tyrosine and/or tryptophane residues is also suggested by the circular dichroism data of Murphy (1971) using the ATP analog 6-mercaptopurine ribonucleoside triphosphate bound to actin.

While there is a probable explanation for the quantum yield decrease, it is more difficult to propose a mechanism for the

increase in lifetime which is coupled to a decreased fluorescence yield. Certainly, if the binding site on actin should involve non-polar residues and/or if the site is "buried" resulting from binding, the lifetime of the bound nucleotide should reflect this, i.e. the lifetime of bound εATP should be longer than the free nucleotide. Although this is compatible with the observed data, the emission spectrum of εATP·G-actin provides little information in this regard since the emission maximum is not sensitive to micropolarity. Additionally, an increase in quantum yield is usually observed when the chromophore is moved to a less polar environment. These considerations suggest that the increase in the lifetime of εATP may result from a shielding from dynamic quenching. This shielding could arise from (1) a rigidly held configuration of the bound nucleotide, (2) a different conformation when εATP is bound, or (3) inaccessibility of the bound nucleotide to quencher molecules that are present in the bulk of the solution. These possibilities are separately discussed below.

If the bound nucleotide is rigidly held at the site, it should have little or no motional freedom of its own. This can be assessed from the following simple calculations. If at the time of absorption the orientation of a rigid fluorophore is defined by its emission dipole, and at the time of emission this dipole has rotated by an angle, ω, due to Brownian notion, this angle can be computed from polarization measurements, using the equation (Weber, 1964):

$$1/P - 1/3 = (1/P_o - 1/3)\,(2/(3\cos^2 \omega - 1)) \qquad (19)$$

where P is the fluorescence polarization, P_o is the fluorescence polarization in the absence of Brownian rotation. Both parameters have been measured. The average free angular rotation from this expression at 20°C is about 40 degrees. On the other hand, the average angular displacement for, under rotational Brownian motion, εATP rigidly attached to an equivalent spherical molecule with M = 46,000 daltons can be calculated from the Einstein equation (Setlow and Pollard, 1962):

$$\theta^2 = (RT/3\eta V)\,\Delta t \qquad (20)$$

where θ^2 is the mean squared value of angle through which the molecule rotates in time Δt, R is the gas constant, T is the absolute temperature, η is the viscosity of the solvent, V is the molar volume. During the lifetime (Δt) of 36 nsec., the average rotation is near 55 degrees. If the attached εATP had a certain degree of motional freedom of its own, then its angular displacement during its excited lifetime would be expected to be greater than 55 degrees, but its displacement calculated from polarization data was only 40 degrees. Therefore, when bound to actin, εATP has little free rotational freedom. The formation of a dark complex was previously postulated to explain the decrease in quantum yield of actin bound εATP. If, on binding to actin, the εATP indeed forms a dark complex and becomes rigidly confined as these simple calculations show, then one would expect a decrease in quantum yield coupled to an increase in lifetime.

A conformational change of εATP on binding to actin is a second possible explanation for its large increase in lifetime. ATP as well as other purine and pyrimidine nucleotides have been shown to favor the anti conformation in solution (Feldman and Agarwal, 1968). As is found for ATP, εATP probably exists in solution in the anti conformation (Figure 19). Although the conformation in solution is not necessarily identical with the conformation when bound, a number of enzymes have been shown to be selective for the anti conformation of nucleotides and will not accept nucleotides in the syn conformation as substrates (Ogilvie et al., 1971; Tavale and Sobell, 1970). It has been shown, however, that the barrier to rotation about the glycosidic bond is much lower for purine nucleotides than for pyrimidine nucleotides (Haschmeyer and Rich, 1967), and the syn conformation may be favored for guanosine in solution. It has been postulated (Kapuler et al., 1970) that a syn $\rightleftharpoons$ anti conformational isomerism is possibly a natural part of various catalytic processes. These considerations suggest that a conformational change for εATP to the syn conformation on binding to actin may be the source of the increased fluorescence lifetime. The lifetimes of ε-nucleotides bound to other proteins have not yet been reported in the literature. But the lifetimes of εADP bound to HMM and of εATP or εADP bound to glutamate dehydrogenase and lactate dehydrogenase are all in the vicinity of 26 nsec. at pH 7 (H. C. Cheung and S. C. Harvey, private communication). Since εATP is known to be a substrate for HMM (Mowery, 1973) and εAMP and εADP are likely to be co-factors

FIGURE 19

Anti and syn conformations of εATP.

ε ATP

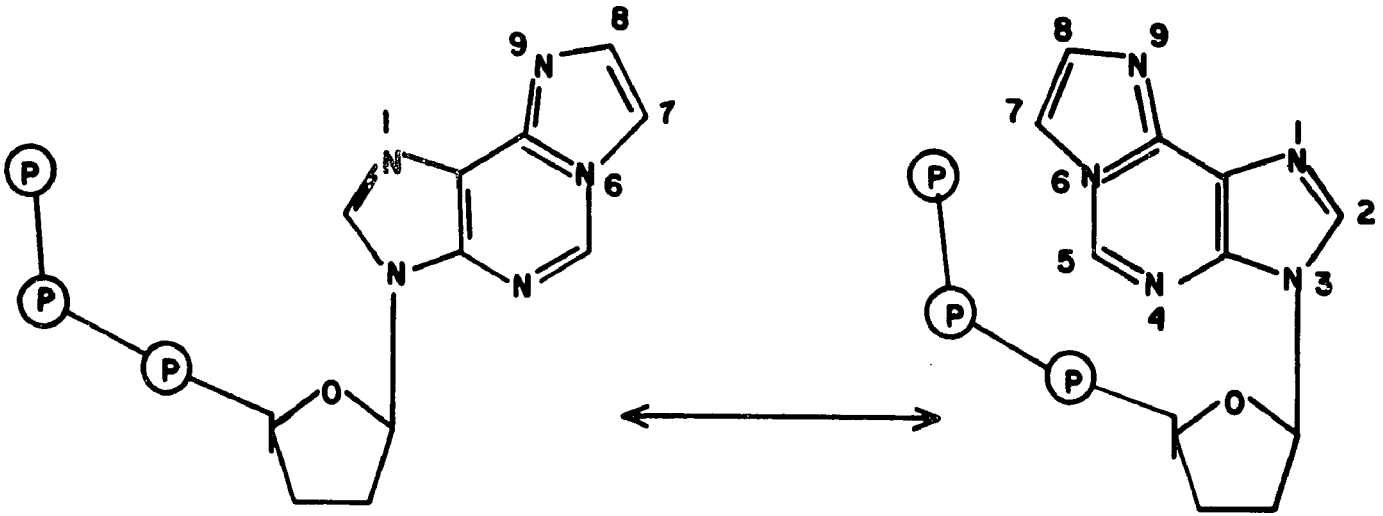

ANTI

SYN

for lactate dehydrogenase (Wicken and Woody, 1974), just as the corresponding natural nucleotides, it is reasonable to think that they are bound in essentially the same anti conformation. This assumption together with the "normal" lifetimes (about 26 nsec.) that were observed points to the possibility that εATP may well be bound to G-actin in a conformation different from the anti conformation.

Recent studies (S. C. Harvey, private communication) indicated that the lifetime of εATP is neither affected by high viscosity, nor by possible quenchers such as oxygen, phosphate or pyrophosphate over a wide range of concentrations. These findings then suggest that the observed lifetime of bound εATP G-actin is unlikely due solely to its being inaccessable to the quenchers in the bulk of solution.

These considerations suggest εATP bound to G-actin to have the following properties. First, the bound nucleotide appears rigidly attached. Second, an interaction with a neighboring residue capable of donating a proton gives rise to a "dark complex". Third, the attached nucleotide may exist in a different conformation than the free nucleotide and this new conformation is maintained as long as it stays bound. Since it is known that in the presence of excess ATP the bound ATP can exchange with free ATP and since it was found in this work that in the presence of ATP the εATP bound to G-actin also exchanges with the ATP (determined by following the fluorescent polarization of a εATP·G-actin solution as a function of time after addition of ATP), it would appear that the nucleotide binding site of G-actin undergoes a

dynamic change in conformation. This change results in the observed exchange of nucleotides. When εATP·G-actin polymerizes, the lifetime decreases from 36.0 to 33.0 nsec. (a t-test on the difference of the means is significant with $p < .01$; $t = 11.33$; $N = 30$) with a concomitant reduction of quantum yield by 25%. It appears reasonable to explain these emission changes by the same processes that take place when εATP binds G-actin. Thus, the changes in lifetime and quantum yield resulting from polymerization can be taken as indications of conformation changes which occur on the G-actin monomer when it polymerizes. The small decrease in the fluorescence lifetime which occurred when εADP·F-actin binds to HMM is proportional to the extent of saturation (30.5 nsec. for a 6:1 complex and 29.2 nsec. for a 1:1 complex). This decrease may reflect either conformational changes occurring in the F-actin on binding to HMM and/or increased accessibility of the bound εADP to quenchers. Further studies would be necessary to determine the alteration in the structure of the ε-nucleotide on binding to actin.

Nuclear magnetic resonance studies could elucidate the conformation of actin-bound εATP. Of interest also is the orientation of the pyrophosphate chain relative to the purine ring. Additional experiments would be required to permit an assessment of the electronic alterations producing the longer lifetimes. One possibility lies in the degree of planarity of the ε-adenine base. X-ray diffraction techniques (Rubin et al., 1972) indicated that adenine bases are not strictly planar. The

angle between the pyrimidine and the imidazole ring is about 2.2 degrees in the crystalline state. An increase in planarity resulting from a more rigid compact conformation such as the syn conformation might yield longer fluorescent lifetimes. Another mechanism resulting from either a conformational change of the εATP or a proximity interaction with residues on the actin is E-type delayed fluorescence.

E-type delayed fluoresence (Parker, 1968) was first investigated with solutions of eosin. In molecules such as eosin which show the delayed fluorescence, the excited molecules can pass into the triplet state from which emission is unlikely. By thermal activation the molecules can return to the fluorescent state and ultimately emit fluorescence. The emission of this fluorescence would thus be delayed by the passage into the triplet state giving an increased fluorescence lifetime. Since the fluorescence energy level is unchanged there will be no shift in the fluorescence emission maximum which is the case for εATP bound to actin. A factor which argues against E-type delayed fluorescence in the case of εATP bound to actin is that previous examples of delayed fluorescence lifetime have been comparable to phorphorescence lifetimes. On binding to actin, the εATP energy levels could be altered so as to favor intersystem crossing into the triplet state to the extent that the fluorescence lifetime is increased by only 30% as observed. One way to investigate this possibility is to measure the fluorescence lifetimes of εATP in the presence of triplet state quencher. Another possibility of interelectronic

level mixing is that of interaction of the fluorescent excited state with some other electronic state which lies between the fluorescent and ground states. There could, for example, be interaction between the fluorescent excited state and a higher vibrational level of the ground state. As long as the interaction energy is small, the mixing of levels will not alter to any great extent the fluorescence spectrum.

C. Fluorescence Polarization Studies of G-actin and F-actin

It is possible to learn something of the size and shape of protein molecules by studying their Brownian rotational motion. For large molecules, information about the Brownian motion must be inferred from a study of the physical properties of the solution. When the dissolved molecules are fluorescent, a study of the polarization of the emitted radiation can give important information about rotational motion. Figure 20-A-top shows a representation of protein molecules in solution with the straight line indicating some fixed direction. If at some time, attention is restricted to those molecules where the given direction happens to coincide (B of Figure 20) and observe these molecules only, then within a very short time they will become randomly oriented; but, if the time interval of observation is short enough they may be observed in a state represented by C of Figure 20 where randomization is not yet complete. If the angle defined by the original direction in B and the new direction in C is called θ,

FIGURE 20

Schematic representation of molecules in solution.

REPRESENTATION OF MOLECULES IN SOLUTION

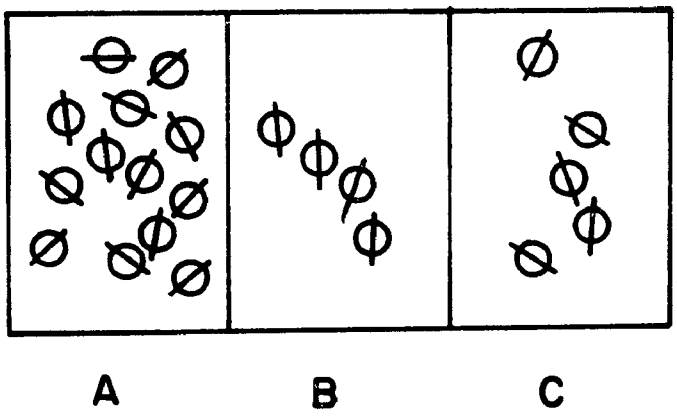

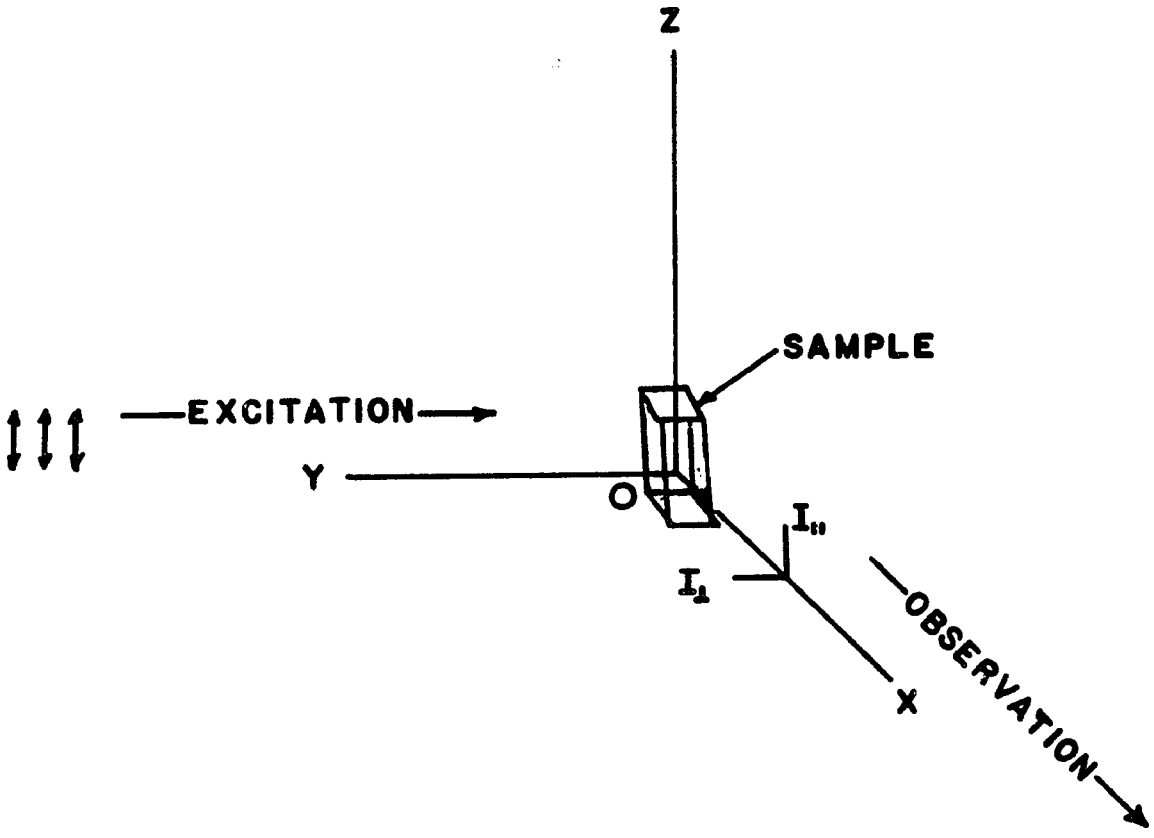

the mean value of its cosine, $\overline{\cos}\ \theta$, can be used as a measure of the angular displacement. $\overline{\cos}\ \theta$ is unity at the initial instant when they are all aligned and reaches zero when the orientation becomes random again. State C can be defined by choosing the $\overline{\cos}\ \theta = 1/e = 0.365$. The time necessary to pass from state B to state C is called the relaxation time of the system (ρ_o). ρ_o is related to the rotational diffusion coefficient D by $\rho_o = 1/2\ D$. The rotational relaxation time has meaning only for stated values of temperature and viscosity.

If the molecules are fluorescent, or have rigidly attached fluorescent probes, the rotational relaxation time may be determined by measuring the polarized fluorescence at right angles to the excitation. Let the solution be illuminated with a beam of plane polarized light in the vertical or OZ direction as shown in Figure 20 (bottom). The cuvette containing the solution of fluorescent molecules is placed at the origin and the emitted radiation observed along the perpendicular direction OX. The absorption and emission of light is connected with fixed directions of the molecules, the oscillators of absorption and emission. The molecules will absorb the exciting light greatest if the direction of their absorption oscillators is parallel to the plane of vibration of the exciting radiation. Therefore, the excited molecules are represented by state B of Figure 20 (top), because from the randomly oriented molecules of the liquid, the excitation has selected those oriented around a particular direction. Each molecule emits a plane polarized wave parallel to its emission

oscillator, and if all molecular directions at the time of emission are equally probable the fluorescent light will be unpolarized. If, however, the orientation that prevailed at the time of the excitation is partially preserved, the fluorescent light will show partial polarization. The interval between excitation and emission for small molecules in water is of the order of 10^{-8} second, while their rotational relaxation time is less. It may be expected that by the time the emission takes place, random orientation of the excited molecules will have occurred leading to unpolarized fluorescence. A large molecule such as a protein, however, will have undergone only a small rotation due to its Brownian movement during a time interval of the order of 10^{-8} second. Consequently, the fluorescent light which it emits will be partially polarized. The higher the viscosity of the medium, and the lower the temperature, the less will be the amount of rotational motion and the greater the polarization. Thus, the study of the polarization of fluorescent light media of varying viscosity and temperature permits an estimate of rotary mobility under Brownian motion, which gives information concerning molecular size and shape.

If the incident light is polarized in the vertical direction OZ, and the emitted light is detected in the direction perpendicular to the exciting light ($I_\perp$) and in the parallel direction ($I_\parallel$), the degree of polarization P is

$$P = \frac{I_\parallel - I_\perp}{I_\parallel + I_\perp}$$

Another quantity related to the polarization is the polarization anisotropy, r, defined as

$$r = \frac{I_{\parallel} - I_{\perp}}{I_{\parallel} + 2I_{\perp}}$$

It is customary to compare the observed harmonic mean of the relaxation time, ρ_H, with the corresponding ρ_o expected for an equivalent spherical molecule. A ratio in excess of unity is indicative of large asymmetry relative to the spherical.

The fluorescence polarization data (Figure 15) indicated a low degree of asymmetry for εATP·G-actin, (ρ_H/ρ_o = 60 nsec./ 40 nsec. = 1.5), while the plot for εADP·F-actin had a zero slope showing that the bound probe senses no rotational freedom in F-actin in the temperature range 5 - 30°C. These conclusions are in agreement with findings by other investigators using fluorescence labeling (Cheung and Morales, 1969). The limiting polarization (P_o = 0.19) for F-actin is considerably smaller than for G-actin (P_o = 0.30), and this depolarization in F-actin could be due to migration of excitation energy among the bound nucleotide in the polymer.

In the single photon technique, fluorescence polarization is studied as a function of time immediately after excitation. First, a fluorescent probe with a suitable excited state lifetime is bound to an interesting site on a macromolecule. Then the probe is excited with a light pulse of short duration (a few nanoseconds), and the polarization or anisotropy of its emission is measured as an explicit function of time in the nanosecond

range. The nanosecond approach complements steady state polarization methods. The steady state method is less direct, since ρ cannot be obtained from a single experiment. A second advantage of the nanosecond approach is that the presence of more than one rotational relaxation time can more easily be detected by it than with the steady state method. Nanosecond fluorescence measurements can also reveal whether a conformational transition occurs in the time interval of nanoseconds.

For a spherical molecule the fluorescence anisotropy has already been expressed by equation 17, [$r(t) = r_o e^{-t/\phi}$]. For rigid ellipsoids, r(t) decays as the sum of three exponential terms (Belford et al., 1972). If the absorption and emission dipoles are fixed relative to the molecular coordinate system,

$$r(t) = r_o \sum_{i=1}^{3} f_i \, e^{-t/\phi i} \qquad (21)$$

where f_i is a factor which depends on the angles between the emission dipole and the ellipsoidal axes. The three ϕ_i's depend on the axial ratio of the ellipsoid as well as on the relation $\phi_o = \eta V/RT$. If the emission oscillators in a collection of molecules are randomly oriented with respect to the ellipsoidal axes, equation 21 reduces to a sum of two exponentials.

Although it is possible to distinguish 3 rotational correlation times according to equation 21, in practice the observed anisotropy data have limited precision and extend only over one order of magnitude. Frequently for large and asymmetrical

molecules, one correlation time is considerably longer than the others and is of the order of microseconds or longer, so that it is not experimentally accessible. Thus in many cases, if the fluorescence probe is randomly attached to a macromolecule only one correlation time is observed. The anisotropy data shown in Figure 16 are analyzed by a single exponential.

As is the case for steady state measurements on εADP·F-actin the anisotropy for this long polymer in low salt (0.1 M KCl) is flat indicating a very large rotational relaxation time.

D. Interaction of F-actin with Heavy Meromyosin

Although it is theoretically possible to see three exponential anisotropy decays for a rigid ellipsoid, the anisotropy plots of εADP·F-actin and the complex of εADP·F-actin plus HMM have a motion in solution that can be fitted by a single exponential decay (Figure 18) in a high salt (0.6 M KCl) solvent. F-actin in low salt (0.1 M KCl) usually shows a flat decay curve indicative of the fact that F-actin is a large asymmetric molecule with a correlation time too large to measure (see Figure 16). In high salt (Figure 18) the F-actin may be depolymerized somewhat to yield a mixed solution of mostly F-actin with some G-actin. This mixture of actins gives the nonflat single decay time. Addition of HMM to G-actin in the absence of ATP has been shown to cause polymerization of the actin, and if the G-actin is labeled with a fluorescent probe, the resulting HMM-F-actin complex exhibits

a zero slope in the Perrin-Weber plot (Cheung et al., 1971). Therefore, addition of HMM to the mixture of G-actin and F-actin would be expected to (1) increase the extent of polymerization, and (2) to form a complex with F-actin resulting in a flat anisotropy plot. On the contrary, the anisotropy plots for the complex of εADP·F-actin with HMM in a molar ratio of 6:1 (actin : HMM) had a greater slope than that of εADP·F-actin alone. At the 6:1 ratio, about 34% of the actin sites are complexed with HMM, since each HMM has two active fragments. HMM apparently induces a rotational degree of freedom in the F-actin polymer. This induced rotational freedom in F-actin is abolished if the F-actin is fully saturated with HMM (the top curve in Figure 18).

The above observation on the 6:1 complex verifies a similar observation from quasielastic scattering of laser light (Fujime, 1970; Fujime et al., 1972; Oosawa, 1973). The laser light scattering studies have also shown that addition of HMM to F-actin renders the F-actin polymer flexible with maximum flexibility occurring at an actin to HMM molar ratio of 6:1. On addition of tropomyosin the ratio of actin to HMM for maximum flexibility decreased from 6:1 to 3:1. The tropomyosin, therefore, appears to modify the cooperative ability of the actin molecules.

The significance of this induced flexibility by HMM cannot be fully understood at this time. Since the interaction *in vivo* between the actin filament and myosin head leads to contraction, the flexibility of the F-actin polymer induced by the same interaction *in vitro* might be indicative of a functional role which

actin plays in the contractile process. Further studies needed to further explore the role of actin in terms of this induced flexibility should include a system containing the regulatory proteins, troponin and tropomyosin, and the effect of Ca^{++} in such a reconstituted system. Such studies would provide an answer based on physical measurements to the question as to whether or not actin monomers indeed communicate with each other via tropomyosin.

As discussed in the Introduction, one tropomyosin and one troponin molecule are associated with six or seven actins in the thin filament. Activation of vertebrate muscle is triggered by the binding of Ca^{++} to a troponin molecule which presumably interacts with tropomyosin causing the tropomyosin to move farther in toward the groove of the F-actin double helix allowing the myosin heads to interact with the actin. The interaction of the myosin heads with actin results in force generation with the energy being supplied by ATP (bound to the myosin head). Normally, therefore, the interaction of actin and myosin occurs in the presence of ATP and is regulated by the presence or absence of Ca^{++}. There is a complicating observation (Bremel and Weber, 1972) which necessitates that the above simplified model of the movement of the tropomyosin in response to the binding of a Ca^{++} by troponin be modified. The presence of rigor complexes, i.e., complexes between myosin and F-actin decorated with a full complement of troponin and tropomyosin appears to exert an effect on contractile activities (as reflected by ATPase activities). At low levels of ATP and when

the number of such complexes is large, no Ca^{++} is needed for ATPase activity. The Ca^{++} sensitivity returns only when the number of such complexes is reduced. In other words, the thin filament is turning on in the absence of calcium, provided that the number of rigor complexes is large. Furthermore, when the number of rigor complexes is large the arrival of Ca^{++} enhances the contractile activity. This enhancement is proportional to the number of rigor complexes already present. These observations imply that there has to be communication between actin molecules. This raises the question of whether or not the actins are communicating directly with one another or through tropomyosin with which they are closely associated. It was concluded by these authors that the communication between the actins required the presence of tropomyosin either as the carrier itself, or to modify the actins, so that in the presence of tropomyosin the actins can communicate. In fact, no communication was found between actins in actomyosin in the absence of added tropomyosin.

We can use the properties of bound εADP in F-actin to test the above ideas. In the actomeromyosin complex that was studied no tropomyosin or troponin was added, but these complexes were just the rigor complexes. The interaction of one actin monomer in F-actin with HMM is sensed by the bound εADP associated with this actin. This εADP then should have a lifetime different from the lifetime of other bound εADP associated with uncomplexed actin monomers. If this complexed monomer is able to communicate with neighboring monomers, then the bound εADP in the uncomplexed

monomers should reflect this communication and would be expected to change its lifetime to that of the complexed monomers. On the other hand if there is no communication, then we would expect to see two sets of lifetimes, one characteristic of the complexed G-monomers and the other characteristic of unbound monomers. The measured lifetimes appear to support the second hypothesis. In uncomplexed F-actin, the lifetime of the bound nucleotide is 33.0 nsec. (Table II). When all of the actin monomers are complexed with HMM, the lifetime decreases to 29.2 nsec. This value can be regarded as the value for bound εADP associated with a complexed actin monomer. If communication exists between the monomers, then in the 6:1 complex (in which about 34% of the monomers are complexed, since each HMM with two heads can complex with two actin monomers) the lifetime of every bound εADP would be expected to become identical and would be 29.2 nsec. However, the measured lifetime was 30.5 nsec., a value between the totally complexed and totally uncomplexed (a t-test on the difference of the means is significant with $p < .01$, $N = 8$). Theoretically, one would expect the lifetime plot to exhibit two exponentials, one giving a lifetime of 33.0 nsec., and the other a lifetime of 29.2 nsec. Such a resolution is not found, however, primarily because of the small difference between the two values. These arguments, which are based on physical measurements, are compatible with Weber's conclusion that there is no direct communication among individual actins.

VI. CONCLUSIONS

1. The fluorescent properties of the bound nucleotide analogs (εATP, εADP), which allow actin to retain its biological function, suggest that εATP or εADP can be used as a structural probe for actin and its interaction with myosin.

2. Fluorescence polarization of εATP·G-actin indicates that the G-actin monomer has a low degree of asymmetry, and that εADP·F-actin in 0.1 M KCl has no measurable rotational mobility with this probe and technique.

3. When the actin monomer polymerizes to εADP·F-actin, the fluorescence lifetime of the rigidly attached ε-nucleotide decreases from 36.0 to 33.0 nsec. while the quantum yield decreased by 25% indicating a change in conformation of the G-actin monomers when it polymerizes.

4. An εADP·F-actin-HMM complex in a 1:1 molar ratio shows no measurable mobility. However, at a molar ratio of 6 to 1 the attached HMM induces a measurable mobility in the F-actin polymer. This induced mobility is absent in the 1:1 complex.

5. Lifetime measurements on acto-HMM complexes suggested that the property of a monomer in the F-actin polymer is to be independent of the other monomers when the F-actin binds HMM. This finding implies that there is no direct structural communication among the monomers in F-actin.

VII. SUGGESTIONS FOR FUTURE WORK

1. To test the possibility of an anti $\rightleftharpoons$ syn conformational change as an explanation for the lifetime increase when εATP binds to actin, two compounds are of interest: guanosine (Haschemeyer and Rich, 1967) and 8-bromoadenosine (Tavale and Sobell, 1970) are believed to exist in the syn conformation in solution. Therefore, the fluorescent lifetime of the ε-derivatives of these two compounds should help decide if the syn-anti transformation is the origin of the increased lifetime.

2. The importance of the double ring structure of the purine bases as in εATP or their planarity could be determined by binding the ε-derivative of a pyrimidine triphosphate, such as cytosine triphosphate to actin.

3. If the longer lifetime of εATP on binding is caused by excited singlet-triplet mixing as in E-type delayed fluorescence, then triplet state quenchers should decrease the fluorescent lifetime of εATP bound to actin. Since the emission of E-type delayed fluorescence is the result of thermal activation of molecules from the lowest triplet state to the first excited singlet state followed by fluorescence, the lifetime would be a function of temperature if E-type delayed fluorescence is responsible for the lifetime increases.

4. Future fluorescence anisotropy studies needed to explore the role of actin in terms of its flexibility should include a system containing the regulatory proteins, troponin and tropomyosin, and the effect of Ca^{++}. The interaction of this system with HMM might give information of the functional role which actin plays in the contractile process.

VIII. REFERENCES

Abe, S., and Maruyama, K. Effect of α-Actinin on F-actin. J. Biochem., 73, 1205-1210 (1973).

Adelstein, R. S., and Conti, M. A. The Characterization of Contractile Proteins from Platelets and Fibroblasts. Cold Spring Harb. Sym. on Quant. Biol., XXXVII, 599-605 (1973).

Asakura, S. The Interaction Between G-actin and ATP. Arch. Biochem. Biophys., 92, 140-149 (1961).

Asakura, S., Taniguchi, M., and Oosawa, F. The Effect of Sonic Vibration on Exchangeability and Reactivity of the Bound Adenosine Diphosphate of F-actin. Biochim. Biophys. Acta, 74, 140-142 (1963).

Bailin, G., and Barany, M. A Simple Procedure for the Preparation of Tropomyosin-Free F-actin. J. Mechanochem. Cell Motility, 1, 189-190 (1972).

Barany, M., Tucci, A. F., and Conover, T. E. The Removal of the Bound ADP of F-actin. J. Mol. Biol., 19, 483-502 (1966).

Belford, G. G., Belford, R. L., and Weber, G. Dynamics of Fluorescence Polarization in Macromolecules. Proc. Nat. Acad. Sci., 69, 1392-1393 (1972).

Boaz, H., and Rollefson, G. K. The Quenching of Fluorescence. Deviation from the Stern-Volmer Law. J. Am. Chem. Soc., 72, 3435-3445 (1950).

Bremel, R. D., and Weber, A. Cooperation Within Actin Filament in Vertebrate Skeletal Muscle. Nature (New Biology), 238, 97-100 (1972).

Carsten, M. E., and Mommaerts, W. F. H. M. A Study of Actin by Means of Starch Gel Electrophoresis. Biochemistry, 2, 28-32 (1963).

Chen, R. F. Fluorescence Lifetime Reference Standards for the Range 0.189 to 115 Nanosecond. Anal. Biochem., 57, 593-604 (1974).

Cheung, H. C., Cooke, R., and Smith, L. The G-Actin → F-Actin Transformation as Studied by the Fluorescence of Bound Dansyl Cystine. Arch. Biochem. Biophys., 142, 333-339 (1971).

Cheung, H. C., and Morales, M. F. Studies of Myosin Conformation by Fluorescent Techniques. Biochemistry, 8, 2177-2182 (1969).

Cohen, L. B. Viscosity of G-ADP and G-ATP Actin. Arch. Biochem. Biophys., 117, 289-295 (1966).

Drabikowski, W., and Gergely, J. The Effect of the Temperature of Extraction on the Tropomyosin Content of Actin. J. Biol. Chem., 237, 3412-3417 (1962).

Ebashi, S. and Endo, M. Calcium Ions and Muscle Contraction. Progr. Biophys. Mol. Biol., 18, 123-183 (1968).

Ebashi, S. E., Kodama, A., and Ebashi, F. Troponin I Preparation and Physiological Function. J. Biochem., 64, 465-477 (1968).

Elzinga, M., Collins, J. H., Kuehl, W. M., and Adelstein, R. S. Complete Amino Acid Sequence of Actin of Rabbit Skeletal Muscle. Proc. Nat. Acad. Sci., 70, 2687-2691 (1973).

Feldman, I., and Agarwal, R. P. Proton Magnetic Resonance Spectra of Adenini 5'-Nucleotides. Assignment of H_2', H_3', and H_4' Resonance Bands and Their Structural Implications. J. Am. Chem. Soc., 90, 7329-7333 (1968).

Fujime, S. Quasielastic Light Scattering from Solution of Macromolecules, II. Doppler Broadening of Light Scattered from Solutions of Semi-Flexible Polymers, F-Actin. J. Phy. Soc. Japan, 29, 751-759 (1970).

Fujime, S., Ishiwata, S., and Maeda, T. F-Actin-Heavy-Meromyosin Complex Studied by Optical Homodyne and Heterodyne Methods. Biochim. Biophys. Acta, 283, 351-363 (1972).

Goll, D. E., Suzuki, A., Temple, J., and Holmes, G. R. Studies on Purified α-Actinin. J. Mol. Biol., 67, 469-488 (1972).

Hanson, J., and Huxley, H. E. The Structural Basis of Contraction in Striated Muscle. Sym. Soc. Expl. Biol., 9, 228-264 (1955).

Harrington, W. F. The Relationship of the Meromyosins to the Molecular Structure of Myosin. J. Biol. Chem. 239, 2822-2829 (1964).

Harvey, S. C., and Cheung, H. C. Computer Simulation of Fluorescence Depolarization Due to Brownian Motion. Proc. Nat. Acad. Sci., 69, 3670-3672 (1972).

Haschemeyer, A. E. V., and Rich, A. Nucleoside Conformation: An Analysis of Steric Barriers to Rotation About the Glycosidic Bond. J. Mol. Biol., 27, 369-384 (1967).

Higashi, S., and Oosawa, F. Conformational Changes Associated with Polymerization and Nucleotide Binding to Actin Molecules. J. Mol. Biol., 12, 843-865 (1965).

Huxley, A. F., and Niedergerke, R. Structural Changes in Muscle During Contraction. Nature, 173, 971-973 (1954).

Huxley, H. E. Electron Microscope Studies of the Organization of the Filaments in Striated Muscle. Biochim. Biophys. Acta, 12, 387-394 (1953).

Huxley, H. E. The Mechanism of Muscular Contraction. Science, 164, 1356-1366 (1969).

Huxley, H. E. Cross-Bridge Movement and Filament Overlap. Biophysical Soc. Abstr., 15th Annual Meeting, 235a (1971).

Huxley, H. E. Structural Changes in the Actin- and Myosin-Containing Filaments during Contraction. Cold Spring Harb. Sym. on Quant. Biol., XXXVII, 361-376 (1973).

Huxley, H. E., and Hanson, J. Changes in the Cross-Striations of Muscle During Contraction and Stretch and Their Structural Interpretation. Nature, 173, 973-976 (1954).

Kapuler, A. M., Monny, C., and Michelson, A. M. The Relationship of Mono- and Polynucleotide Conformation to Catalysis by Polynucleotide Phosphorylase. Biochim. Biophys. Acta, 217, 18-29 (1970).

Kasai, M., Nakano, E., and Oosawa, F. Polymerization of Actin Free from Nucleotides and Divalent Cations. Biochim. Biophys. Acta, 94, 494-503 (1965).

Kasai, M., and Oosawa, F. Behavior of Divalent Cations and Nucleotides Bound to F-Actin. Biochim. Biophys. Acta, 172, 300-310 (1969).

Laki, K., Bowen, W. J., and Clark, A. M. The Polymerization of Proteins. J. Gen. Physiol., 33, 437-443 (1950).

Lowry, O. H., Rosebrough, N. J., Farr, A. L., and Randall, R. J. Protein Measurement with the Folin Phenol Reagent. J. Biol. Chem., 193, 265-275 (1951).

Martonosi, A. Studies on Actin. J. Biol. Chem., 237, 2795-2803 (1962).

Maruyama, K. A New Protein Factor Hindering Network Formation of F-Actin in Solution. Biochim. Biophys. Acta, 94, 208-225 (1965).

Maruyama, K. Instability of F-Actin under the Influence of β-Actinin. Biochim. Biophys. Acta, 305, 679-683 (1973).

Masaki, T., Endo, M., and Ebashi, S. Localization of 6S Component of α-Actinin at Z-Band. J. Biochem., 62, 630-632 (1967).

Masaki, T., and Takaiti, O. M-Protein. J. Biochem., 75, 367-380 (1974).

Masaki, T., Takaiti, O., and Ebashi, S. "M-Substance," A New Protein Constituting the M-Line of Myofibrils. J. Biochem., 64, 909-910 (1968).

Mihalyi, E., and Szent-Gyorgyi, A. G. Trypsin Digestion of Muscle Proteins. J. Biol. Chem., 201, 189-196 (1953).

Miki, M., Ohnuma, H., and Mihashi, K. Interaction of Actin with εATP. FEBS Letters, 46, 17-19 (1974).

Mowery, P. C. Investigations into the Efficacy of εATP as a Substrate for Contractility Studies. Arch. Biochem. Biophy., 159, 394-377 (1973).

Mueller, H., and Perry, S. V. The Degradation of Heavy Meromyosin by Trypsin. Biochem. J., 85, 431-439 (1962).

Murphy, A. J. Circular Dichroism of the Adenine and 6-Mercapto-purine Nucleotide Complexes of Actin. Biochem., 10, 3723-3729 (1971).

Murray, J. M., and Weber, A. The Cooperative Action of Muscle Proteins. Sci. Amer., 230, 58-71 (1974).

Muszbek, L., and Laki, K. Cleavage of Actin by Thrombin. Proc. Nat. Acad. Sci., 71, 2208-2211 (1974).

Nagy, B. Optical Rotatory Dispersion of G-Actin-Adenosine-5'-Diphosphate. Biochim. Biophys. Acta, 115, 498-500 (1966).

Ogilvie, K. K., Slotin, L., and Rheault, P. Novel Substrate of Adenosine Deaminase. Biochem. Biophys. Res. Commu., 45, 297-300 (1971).

Ohtsuki, I., Masaki, T., Nonomura, Y., and Ebashi, S. Periodic Distribution of Troponin Along the Thin Filament. J. Biochem., 61, 817-819 (1967).

Oosawa, F., Fukime, S., Ishiwata, S., and Mihashi, K. Dynamic Property of F-Actin and Thin Filament. Cold Spring Harb. Sym. Quant. Biol., XXXVII, 277-285 (1973).

Parker, C. A. Photoluminescence of Solutions. Elsevier Pub. Co., New York, (1968).

Parker, C. A., and Barnes, W. J. Some Experiments with Spectrofluorimeters and Filter Fluorimeters. Analyst. 82, 606-618 (1957).

Parry, D. A. D., and Squire, J. M. Structural Role of Tropomyosin in Muscle Regulation: Analysis of the X-ray Diffraction Patterns from Relaxed and Contracting Muscles. J. Mol. Biol., 75, 33-55 (1973).

Perrin, F. Polarisation de la Lumiere de Fluorescence. Vie Moyenne des Molecules dans L'Etat Excite. J. Phys. Rad., 7, 390-401 (1926).

Pesce, A. J., Rosen, C., and Pasby, T. L., editors, Fluorescence Spectroscopy. Marcel Dekker, Inc., New York (1971).

Potter, J. D., and Gergely, J. Troponin, Tropomyosin, and Actin Interactions in the Ca^{++} Regulation of Muscle Contraction. Biochemistry, 13, 2697-2703 (1974).

Radda, G. K. Fluorescent Probes in Membrane Studies. Biomembranes, 3, 247-266 (1972).

Rees, M. K., and Young, M. Studies on the Isolation and Molecular Properties of Homogeneous Globular Actin. J. Biol. Chem., 242, 4449-4450 (1967).

Rubin, J., Brennan, T., and Sundaralingam, M. Crystal and Molecular Structure of a Naturally Occurring Dinucleoside Monophosphate. Uridylyl-(3'-5')-Adenosine Hemihydrate. Conformational "Rigidity" of the Nucleotide Unit and Models for Polynucleotide Chain Folding. Biochemistry, 11, 3112-3128 (1972).

Secrist, J. A., Barrio, J. R., and Leonard, N. J. A Fluorescent Modification of Adenosine Triphosphate with Activity in Enzyme Systems: 1,N^6-Ethenoadenosine Triphosphate. Science, 175, 646-647 (1972a).

Secrist, J. A., Barrio, J. R., Leonard, N. J., and Weber, G. Fluorescent Modification of Adenosine-Containing Coenzymes. Biological Activities and Spectroscopic Properties. Biochemistry, 11, 3499-3506 (1972b).

Setlow, R. B., and Pollard, E. C. Molecular Biophysics. Addison-Wiley, Reading, (1962).

Spencer, R. D., Weber, G., Tolman, G. L., Barrio, J. R., and Lionard, N. J. Species Responsible for the Fluorescence of 1,N^6-Ethenoadenosine. Eur. J. Biochem., 45, 425-429 (1974).

Starr, R., and Offer, G. Polypeptide Chains of Intermediate Molecular Weight in Myosin Preparations. FEBS Letters, 15, 40-44 (1971).

Straub, F. B., and Feuer, G. Adenosinetriphosphate the Functional Group of Actin. Biochim. Biophys. Acta, 4, 455-470 (1950).

Strohman, R. C., and Samorodin, A. J. The Requirements for Adenosine Triphosphate Binding to Globular Actin. J. Biol. Chem., 237, 363-369 (1962).

Stryer, L. Fluorescence Spectroscopy of Proteins. Science, 162, 526-533 (1968).

Szent-Gyorgyi, A. G. Meromyosins, the Subunits of Myosin. Arch. Biochem. Biophys. 42, 305-320 (1953).

Tanford, C. Physical Chemistry of Macromolecules. John Wiley and Sons, Inc., New York, (1961).

Tao, T. Time-Dependent Fluorescence Depolarization and Brownian Rotational Diffusion Coefficients of Macromolecules. Biopolymers, 8, 609-632 (1969).

Tavale, S. S., and Sobell, H. M. Crystal and Molecular Structure of 8-Bromoguanosine and 8-Bromoadenosine. Two Purine Nucleosides in the Syn Conformation. J. Mol. Biol., 48, 109-123 (1970).

Taylor, E. W. Chemistry of Muscle Contraction. Ann. Rev. Biochem., 41, 577-616 (1972).

Thames, K. E., Cheung, H. C., and Harvey, S. C. Binding of 1,N^6-Ethenoadenosine Triphosphate to Actin. Biochem. Biophys. Res. Comm., 60, 1252-1261 (1974).

Tonomura, Y. Muscle Proteins, Muscle Contraction, and Cation Transport. University Park Press, Baltimore, Maryland, (1973).

Tonomura, Y., Appel, P., and Morales, M. On the Molecular Weight of Myosin. Biochemistry, 5, 515-527 (1966).

Tonomura, Y., and Oosawa, F. Molecular Mechanism of Contraction. Ann. Rev. Biophy. Bioeng., 1, 159-190 (1972).

Tonomura, Y., Tokura, S., and Sekiya, K. Binding of Myosin A to F-Actin. J. Biol. Chem., 237, 1074-1081 (1962).

Weber, G. Polarization of the Fluorescence of Macromolecules. Biochem. J., 51, 145-155 (1952).

Weber, G. Rotational Brownian Motion and Polarization of the Fluorescence of Solutions. Adv. Prot. Chem., 8, 415-459 (1953).

Weber, G. "Polarization of the Fluorescence of Solutions." In Fluorescence and Phosphorescence Analysis, (ed. D. M. Hercules). Interscience, New York, (1964).

Weber, K., and Osborn, M. The Reliability of Molecular Weight Determinations by Dodecyl Sulfate-Polyacrylamide Gel Electrophoresis. J. Biol. Chem., 244, 4406-4412 (1969).

Weihing, R. R., and Korn, E. D. Acanthamoeba Actin, Isolation and Properties. Biochemistry, 10, 590-600 (1971).

West, J. J. Binding of Adenosine Diphosphate to G-Actin. Biochemistry, 9, 1239-1246 (1970a).

West, J. J. Adenosine Triphosphate and Inosine Triphosphate Dependent Conformational Changes of Adenosine Diphosphate-G-Actin. Biochemistry, 9, 3847-3853 (1970b).

West, J. J. Binding of Nucleotide to Cation-Free G-Actin. Biochem., 10, 3547-3553 (1971).

Wicken, J. S., and Woody, R. W. Conformational Changes in Liver Alcohol Dehydrogenase Upon Nucleotide Binding: Detection by Circular Dichroism of Dye Complexes. Arch. Biochem. Biophys., 162, 12-16 (1974).

Yguerabide, J., Epstein, H. F., and Stryer, L. Segmental Flexibility in an Antibody Molecule. J. Mol. Biol., 51, 573-590 (1970).

GRADUATE SCHOOL
UNIVERSITY OF ALABAMA IN BIRMINGHAM
DISSERTATION APPROVAL FORM

Name of Candidate Kenneth Edwin Thames

Major Subject Physiology and Biophysics

Title of Dissertation Binding of 1,N^6-Ethenoadenosine Triphosphate to Actin Fluorescence Emission Properties

Dissertation Committee:

H. C. Cheung, Chairman

Edwin M. Miller

William J. Butler

Director of Graduate Program Wayne S. Rehm

Dean, UAB Graduate School S B Barker

Date 30 May 1975